The Structure of the

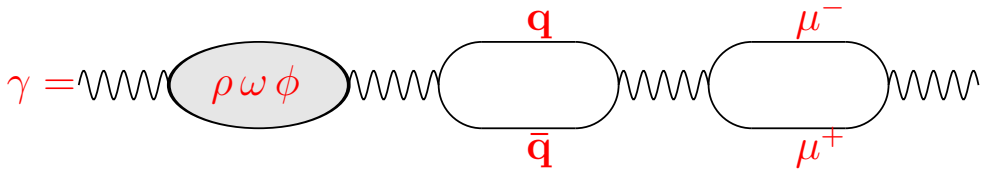

from Deep Inelastic Scattering

Richard Nisius (CERN) Hamburg, 15.12.99

- Introduction

1. Quasi-Real Photons
    1. QED structure
    2. Hadronic structure
2. Virtual Photons
    1. QED structure
    2. Hadronic structure
3. Results from Other Reactions
    1. Photon-Photon Scattering
    2. Results from HERA

- Conclusions

Why do we talk about Photon Structure?

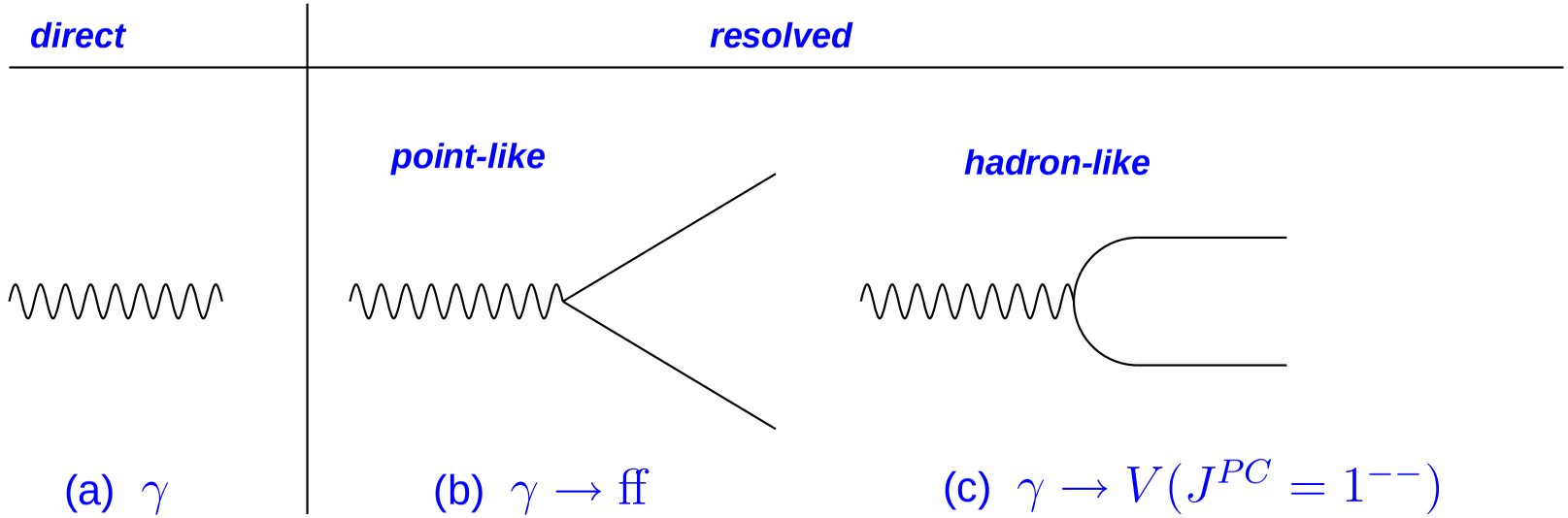

In (a) the whole photon interacts $\Rightarrow$ NO structure

The fluctuations (b,c) exist due to the uncertainty principle $\Rightarrow$ Photon 'Structure'

The typical lifetime of the fluctuations increases with the photon energy and decreases with the photon virtuality

The reaction e e $\longrightarrow$ e e X

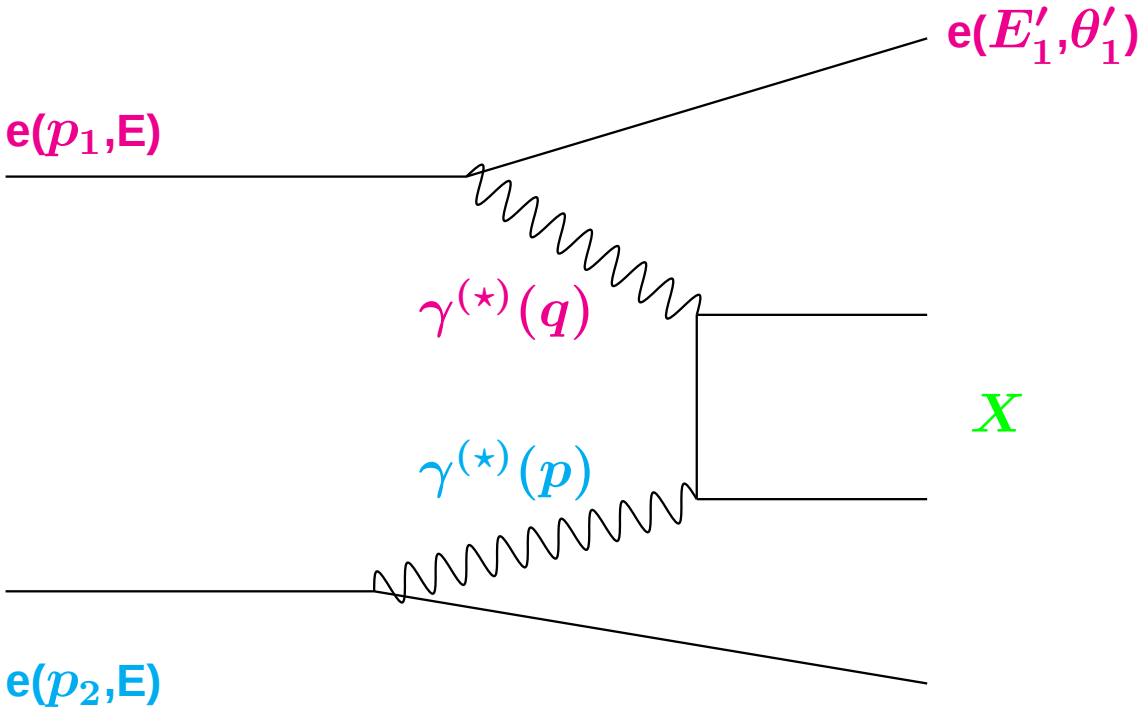

$$
\begin{aligned}
\mathrm{d}^6\sigma &= \frac{\mathrm{d}^3p'_1\,\mathrm{d}^3p'_2}{E'_1E'_2}\,\frac{\alpha^2}{16\pi^4Q^2P^2}\left[\frac{(q\cdot p)^2-Q^2P^2}{(p_1\cdot p_2)^2-m_\mathrm{e}^2m_\mathrm{e}^2}\right]^{1/2} \\
&\Big(4\rho_1^{++}\rho_2^{++}\sigma_{\mathrm{TT}}+2\rho_1^{++}\rho_2^{00}\sigma_{\mathrm{TL}} \\
&+2\rho_1^{00}\rho_2^{++}\sigma_{\mathrm{LT}}+\rho_1^{00}\rho_2^{00}\sigma_{\mathrm{LL}}+ \\
&2|\rho_1^{+-}\rho_2^{+-}|\tau_{\mathrm{TT}}\cos 2\bar{\phi}-8|\rho_1^{+0}\rho_2^{+0}|\tau_{\mathrm{TL}}\cos\bar{\phi}\Big) \\
Q^2 &= -q^2 = 2\,E\,E'_1\,(1-\cos\theta'_1) \\
P^2 &= -p^2 = 2\,E\,E'_2\,(1-\cos\theta'_2) \\
x &= \frac{Q^2}{Q^2+W^2+P^2}
\end{aligned}
$$

The limit of deep inelastic electron-photon scattering

Using:

$$
\begin{aligned}
2xF_{\mathrm{T}}^{\gamma} &= \frac{Q^2}{4\pi^2\alpha}\,\sigma_{\mathrm{TT}}(x,Q^2) \\
F_{\mathrm{L}}^{\gamma} &= \frac{Q^2}{4\pi^2\alpha}\,\sigma_{\mathrm{LT}}(x,Q^2) \\
F_2^{\gamma} &= 2xF_{\mathrm{T}}^{\gamma} + F_{\mathrm{L}}^{\gamma}
\end{aligned}
$$

and the limit $(p\cdot q)^2 - Q^2P^2 \approx (p\cdot q)^2$ the cross section reduces to:

$$
\frac{\mathrm{d}^4\sigma}{\mathrm{d}x\,\mathrm{d}Q^2\,\mathrm{d}z\,\mathrm{d}P^2} = \frac{\mathrm{d}^2N_{\gamma}^{\mathrm{T}}}{\mathrm{d}z\mathrm{d}P^2}\cdot\frac{2\pi\alpha^2}{x\,Q^4}\cdot\left[1+(1-y)^2\right]\cdot \underbrace{\left[2xF_{\mathrm{T}}^{\gamma}(x,Q^2) + \frac{2(1-y)}{1+(1-y)^2}F_{\mathrm{L}}^{\gamma}(x,Q^2)\right]}_{\to F_2^{\gamma}\ \text{for}\ y\ll 1}
$$

with: $$\frac{\mathrm{d}^2N_{\gamma}^{\mathrm{T}}}{\mathrm{d}z\mathrm{d}P^2} = \frac{\alpha}{2\pi}\left[\frac{1+(1-z)^2}{z}\frac{1}{P^2} - \frac{2\,m_{\mathrm{e}}^2\,z}{P^4}\right]$$

The world data on $F_{2,\mathrm{QED}}^{\gamma}$

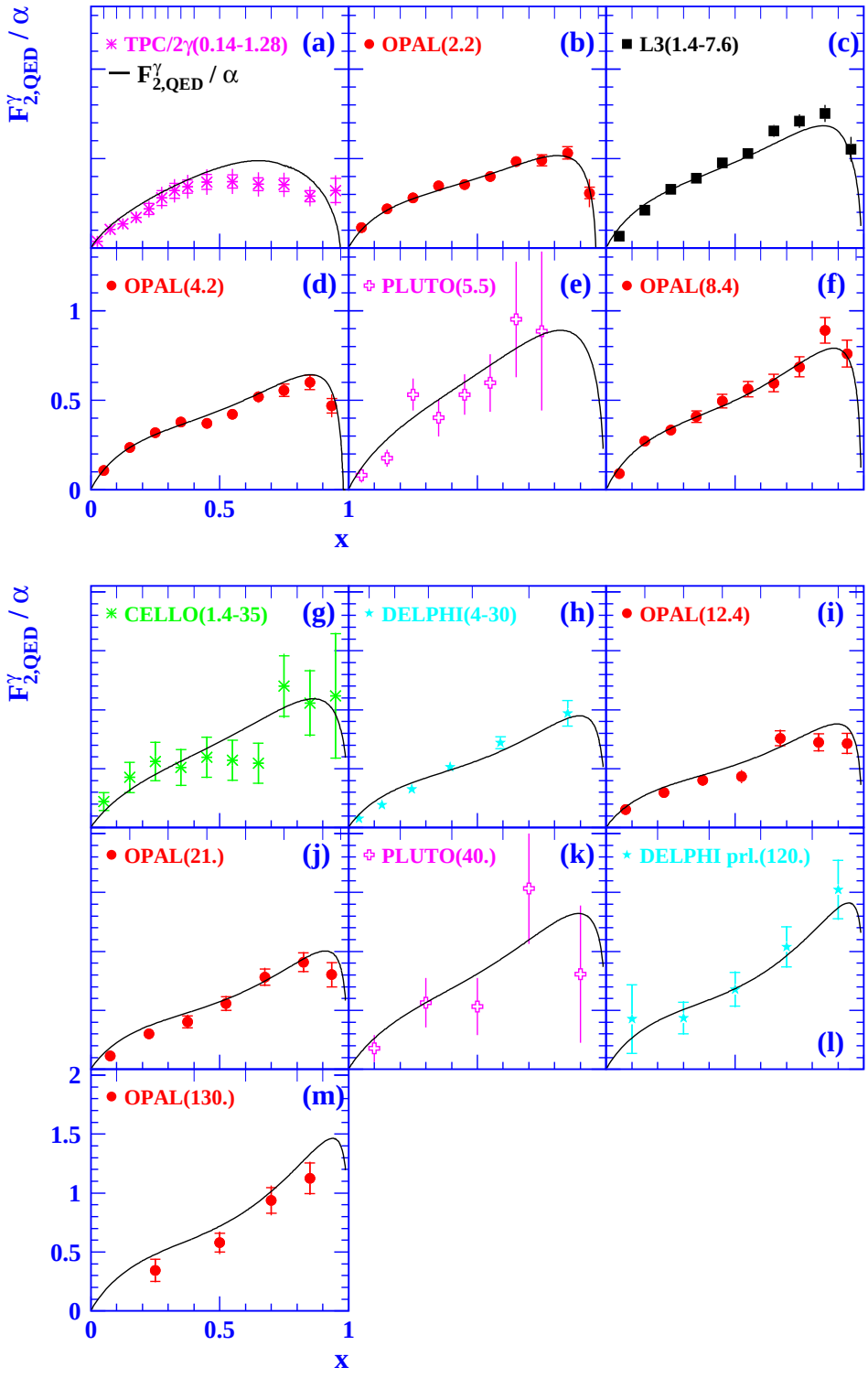

The dependence of $F_{2,\mathrm{QED}}^{\gamma}$ on P^2 and m_μ

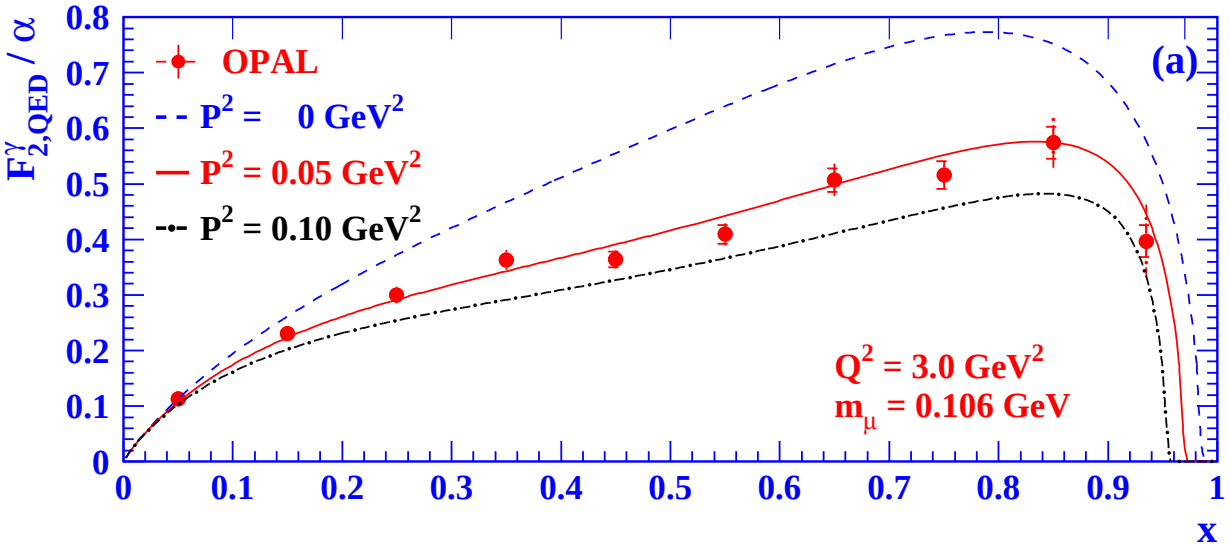

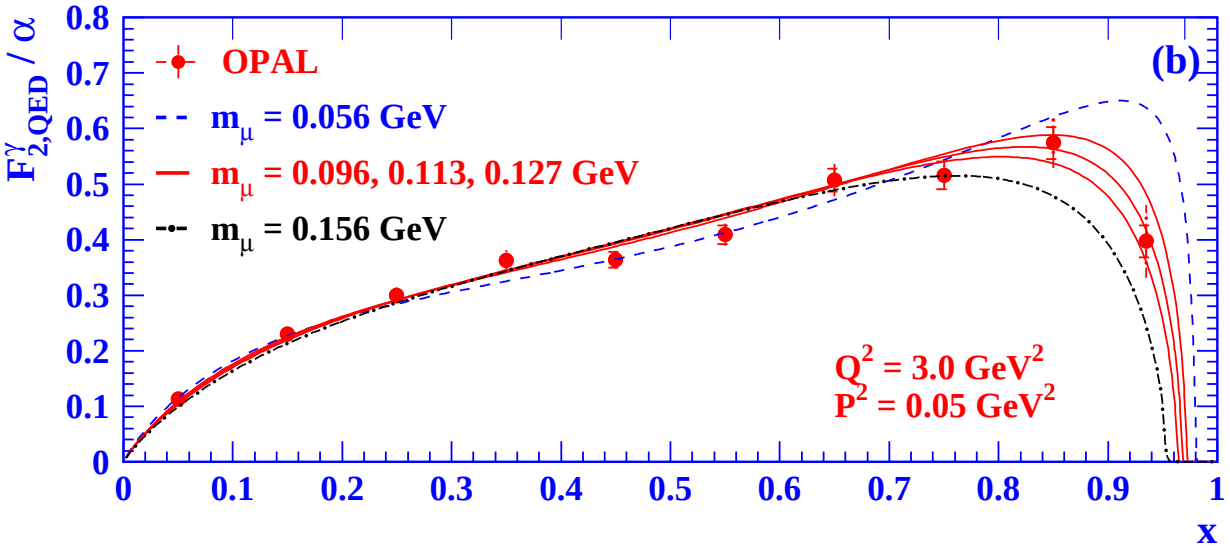

The P^2 dependence is clearly observed in the data.
The muon mass can be determined to about $\pm 15\%$.

Azimuthal Correlations

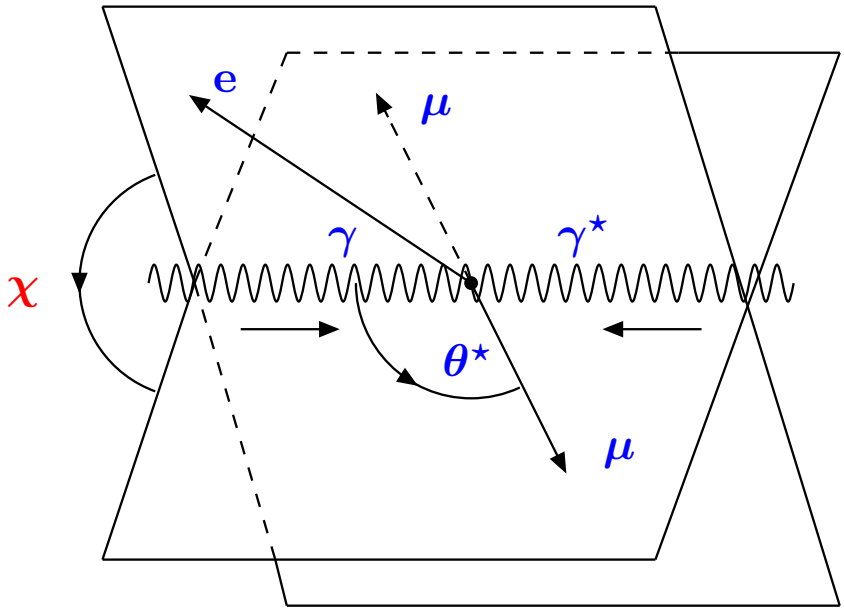

$\mathbf{e\gamma \to e\mu\mu}$

$$\mathrm{d}\sigma \quad \propto \quad 1 - \rho(y) F_{\mathrm{A}}^{\gamma}/F_2^{\gamma} \cos\chi + \frac{1}{2}\epsilon(y) F_{\mathrm{B}}^{\gamma}/F_2^{\gamma} \cos 2\chi$$

$$\epsilon(y) = \frac{2(1-y)}{1+(1-y)^2} \approx 1, \;\; \rho(y) = \frac{(2-y)\sqrt{1-y}}{1+(1-y)^2} \approx 1$$

The χ dependence gives access to other structure functions besides F_2^{γ}.

The functional form of $F_{\rm A}^{\gamma}$ and $F_{\rm B}^{\gamma}$

$$
\begin{aligned}
F_{\rm A}^{\gamma}(x,\beta) &= \frac{4\alpha}{\pi} x\sqrt{x\,(1-x)}\,(1-2x)\left\{\beta\left[1+\left(1-\beta^2\right)\frac{1-x}{1-2x}\right]\right. \\
&\left. +\frac{3x-2}{1-2x}\sqrt{1-\beta^2}\,\arccos\left(\sqrt{1-\beta^2}\right)\right\} \\
F_{\rm B}^{\gamma}(x,\beta) &= \frac{4\alpha}{\pi} x^2\,(1-x)\left\{\beta\left[1-\left(1-\beta^2\right)\frac{1-x}{2x}\right]\right. \\
&\left. +\frac{1}{2}\left(1-\beta^2\right)\left[\frac{1-2x}{x}-\frac{1-x}{2x}\left(1-\beta^2\right)\right]\ln\left(\frac{1+\beta}{1-\beta}\right)\right\} \\
F_{2}^{\gamma}(x,\beta) &= \frac{\alpha}{\pi} x\left\{\left[x^2+(1-x)^2\right]\ln\left(\frac{1+\beta}{1-\beta}\right)-\beta+8\beta x\,(1-x)\right. \\
&\left. -\beta\left(1-\beta^2\right)(1-x)^2\right. \\
&\left. +\left(1-\beta^2\right)(1-x)\left[\frac{1}{2}\,(1-x)\left(1+\beta^2\right)-2x\right]\ln\left(\frac{1+\beta}{1-\beta}\right)\right\} \\
\beta &= \sqrt{1-\frac{4m_\mu^2}{W^2}}\,, \qquad \text{(leading log } \beta\longrightarrow 1\text{)}
\end{aligned}
$$

The improvement of the leading log approximation

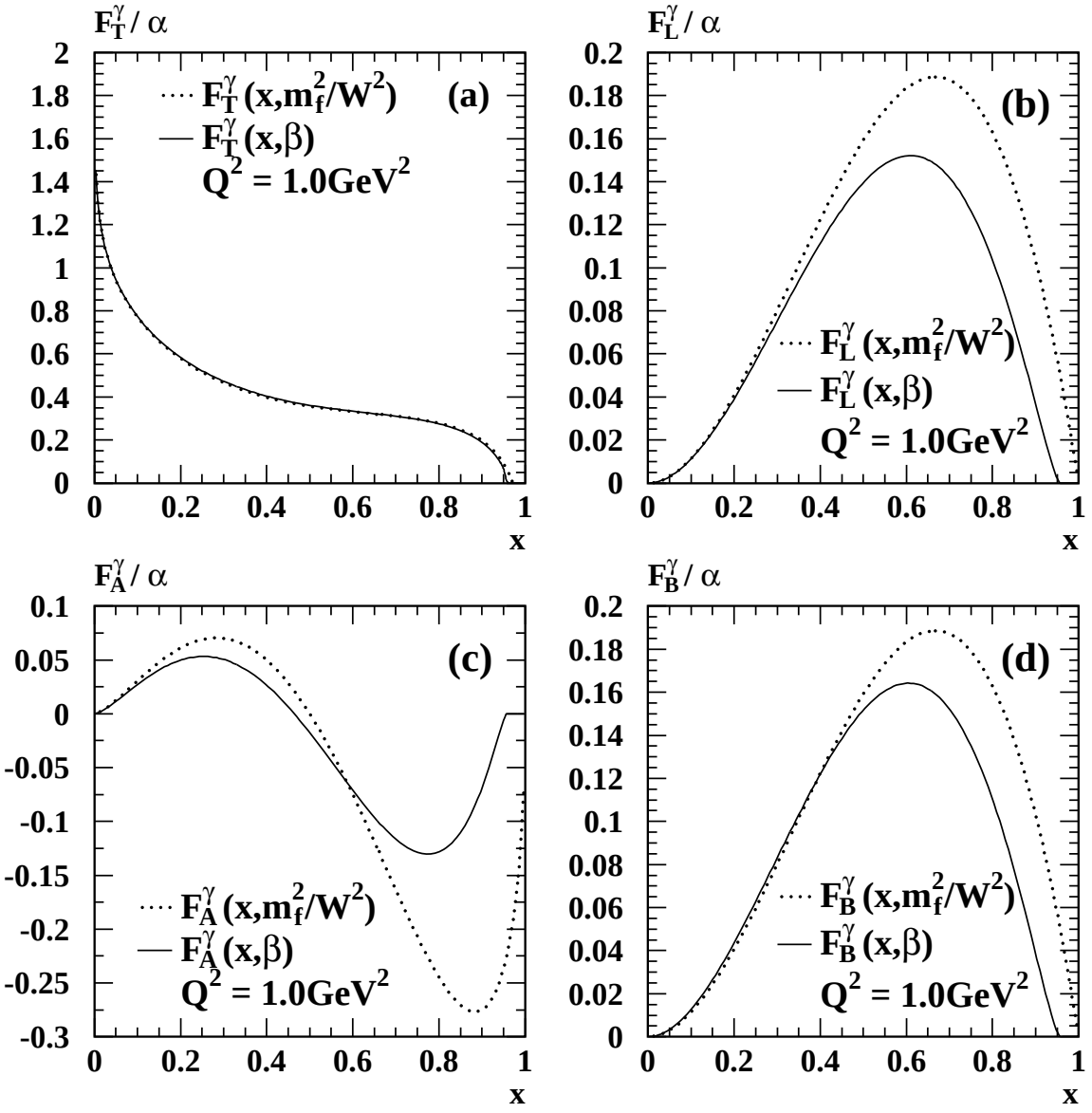

The structure function $F^{\gamma}_{\mathrm{A,QED}}$ and $F^{\gamma}_{\mathrm{B,QED}}$ receive seizable corrections at low values of Q^2

R. Nisius, M.H. Seymour, Phys.Lett. B452 (1999), 409-413

The structure functions F_A^γ and F_B^γ

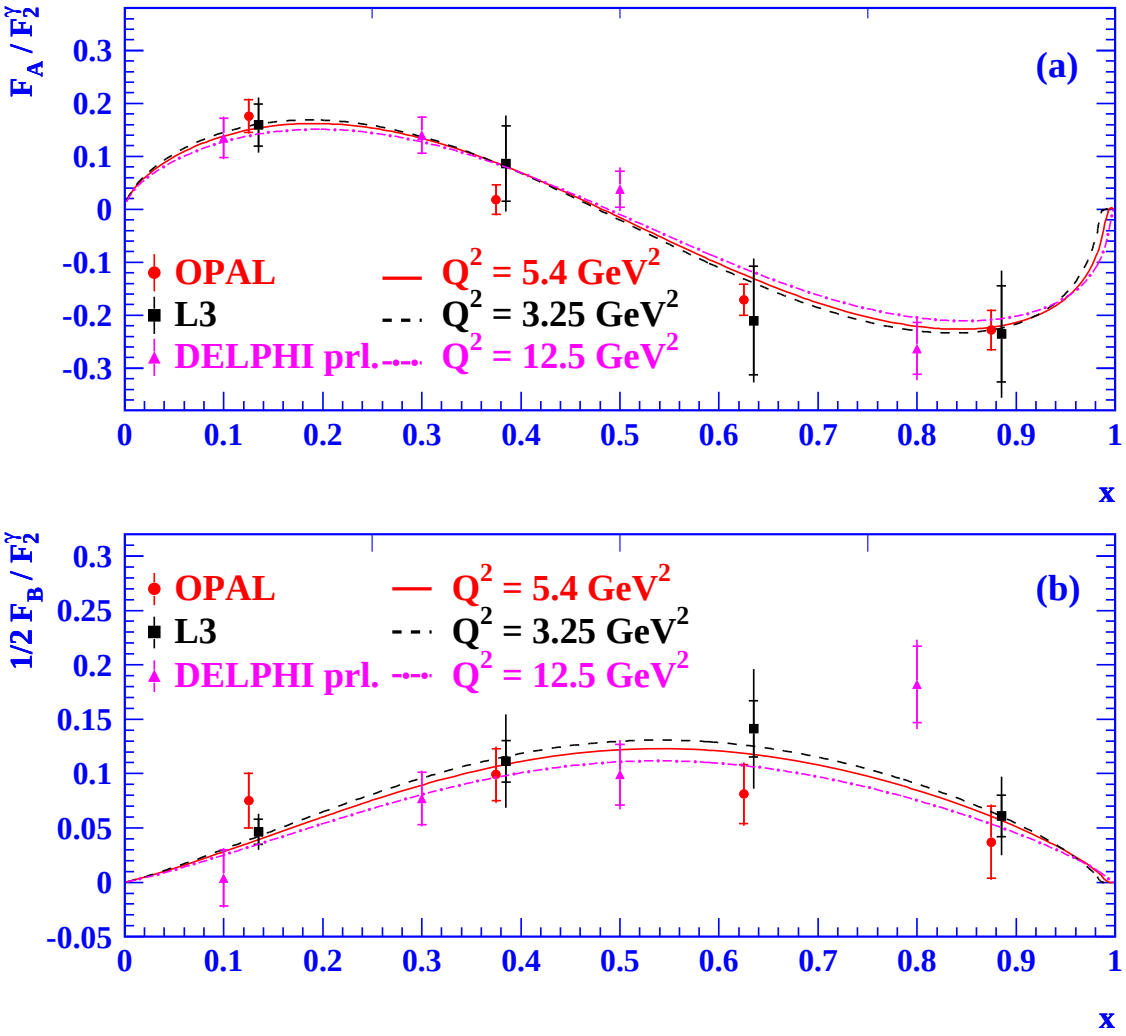

First measurement that goes further than measuring the differential cross-section.

The description of the hadronic final state

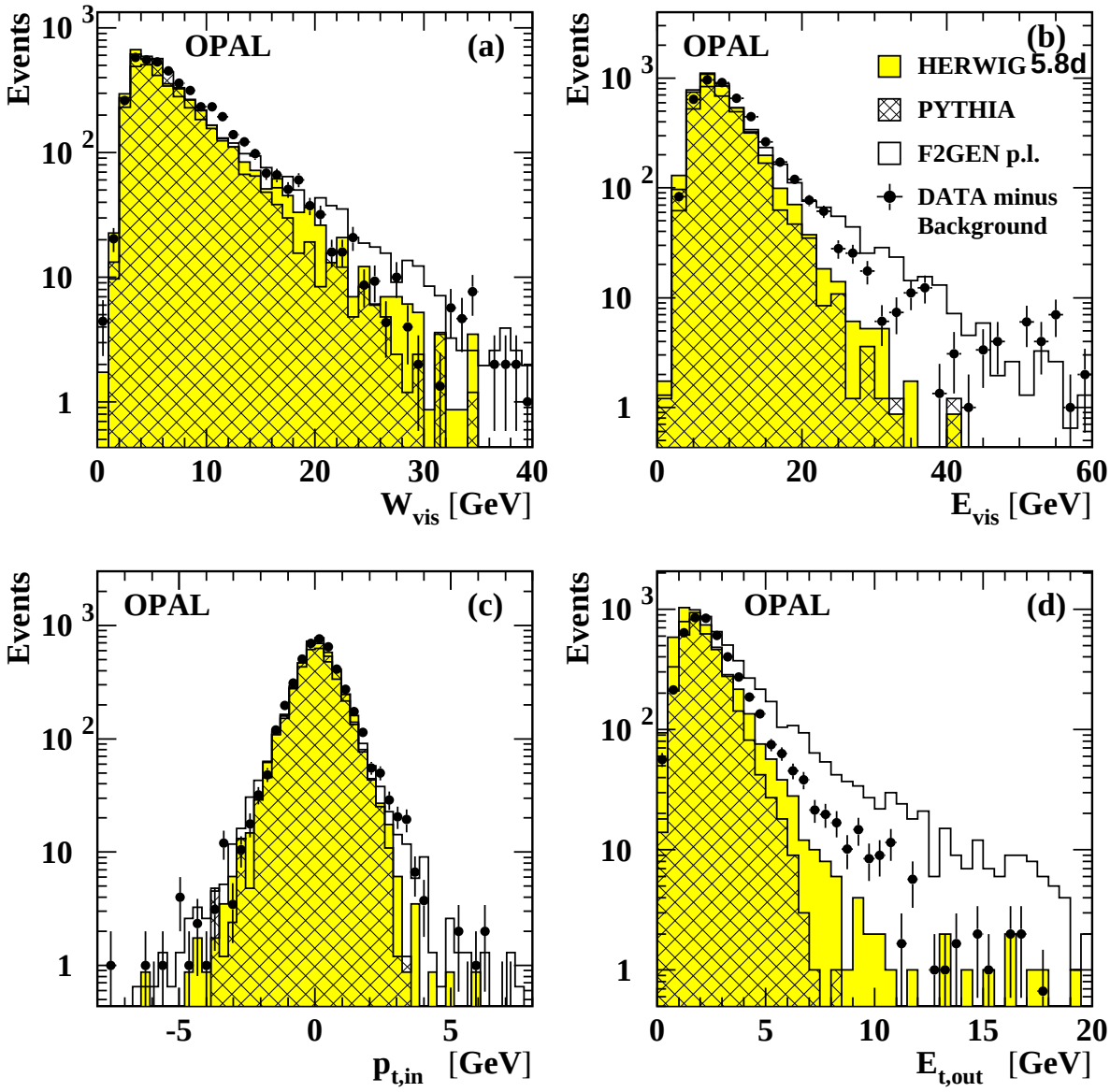

There are significant differences between the data and the Monte Carlo predictions (OPAL '96)

Comparison to LEP combined data

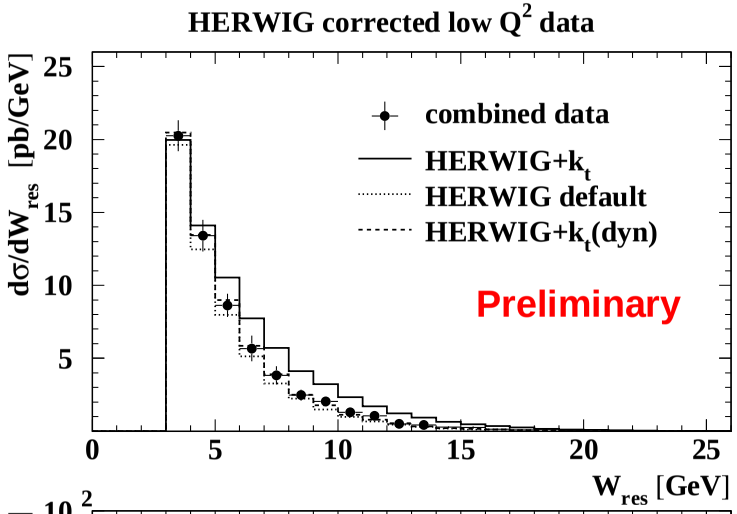

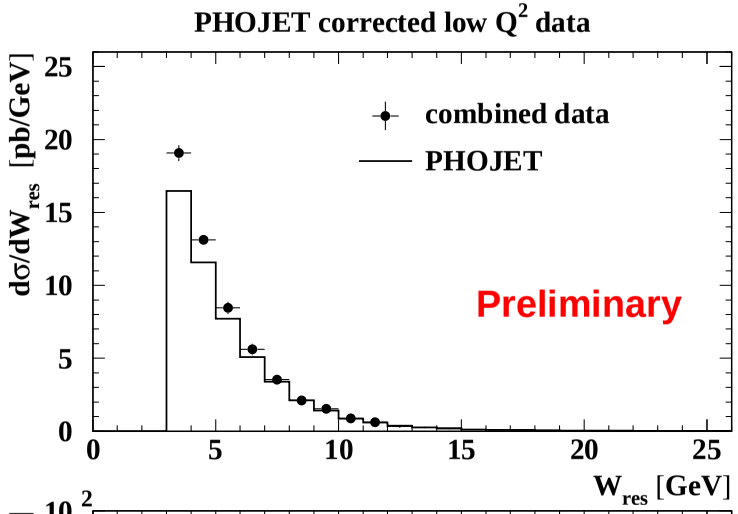

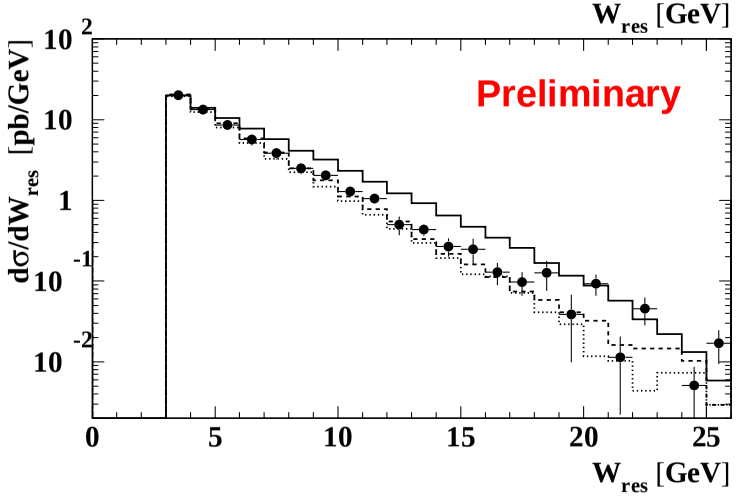

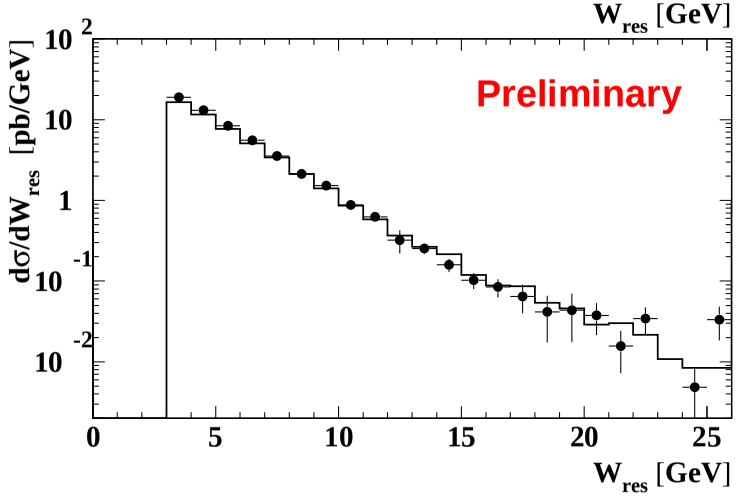

The combined data are a valuable input to constrain the Monte Carlo models (LEP Two-Photon WG '99)

The contributions to $F_2^\gamma(x, Q^2)$

$$F_2^\gamma(x, Q^2) = x \sum_{c,f} e_q^2 \, f_{q,\gamma}(x, Q^2)$$

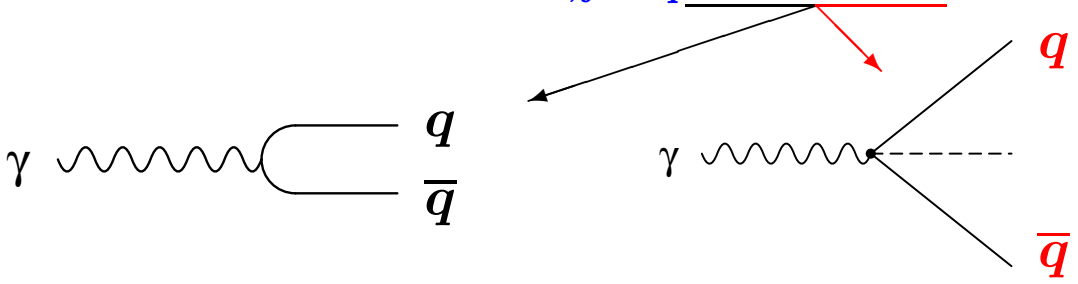

hadron-like, *non–perturbative* **point-like,** *perturbative*

e.g. VMD(ρ, ω, ϕ), low-x **high-x**

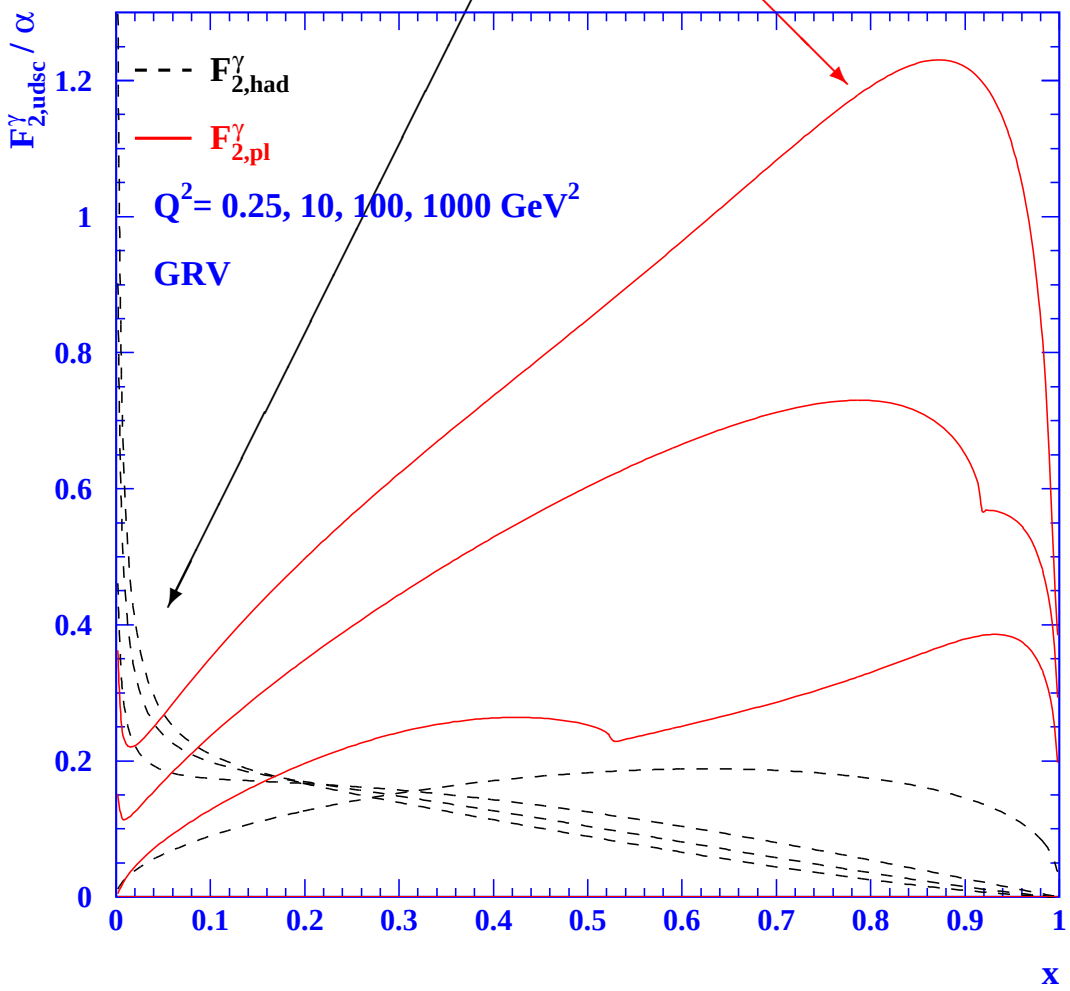

The world data on F_2^γ

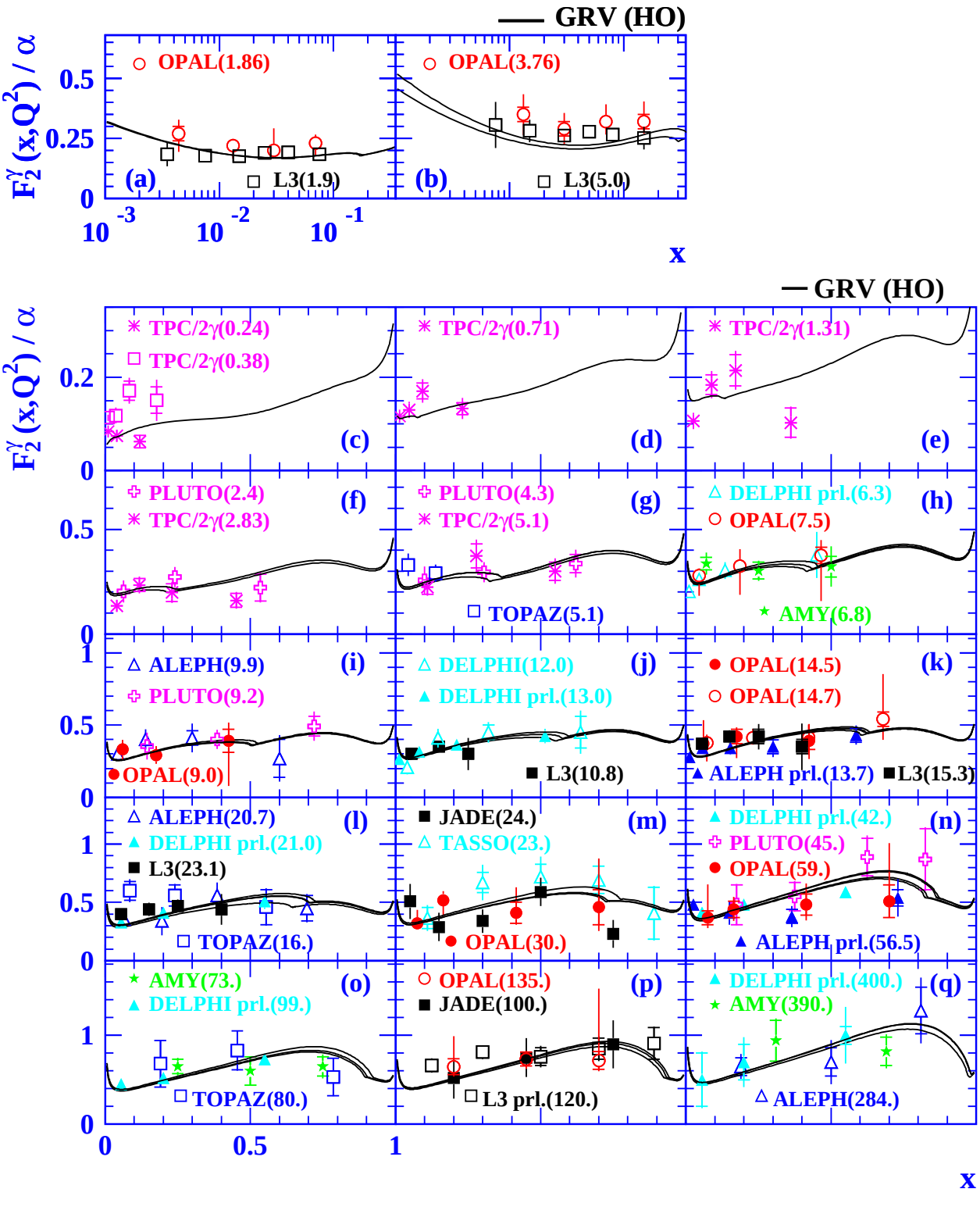

Charm production tagged by D*s

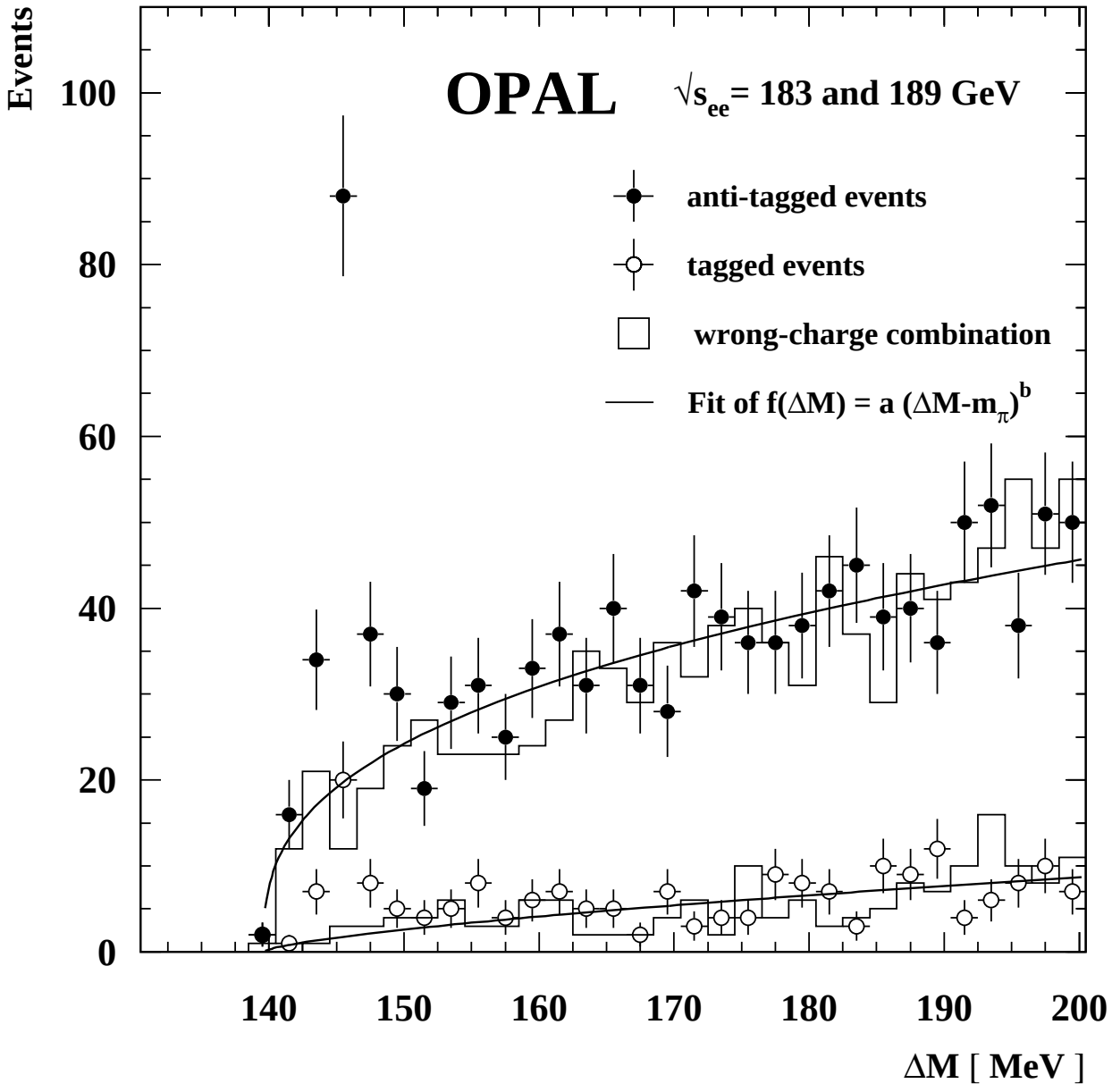

A clear signal in the $\Delta(M) = M(D^{\star}) - M(D^{0})$ mass spectrum is seen for anti-tagged and tagged events

The first measurement of $F_{2,c}^{\gamma}$

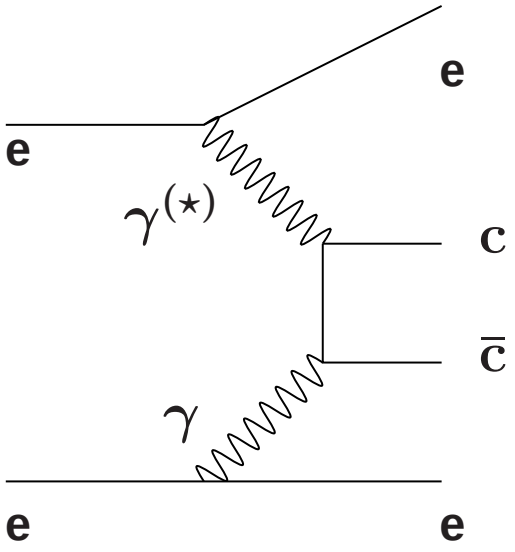

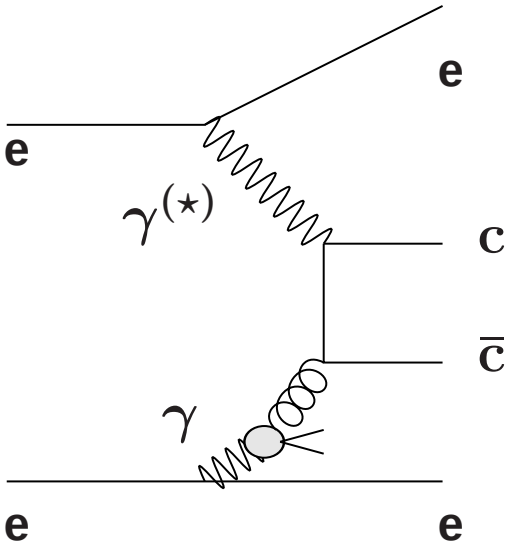

point-like, purely perturbative QCD prediction, dominates at high-x

hadron-like, depends on f_g^{γ}, dominates at low-x

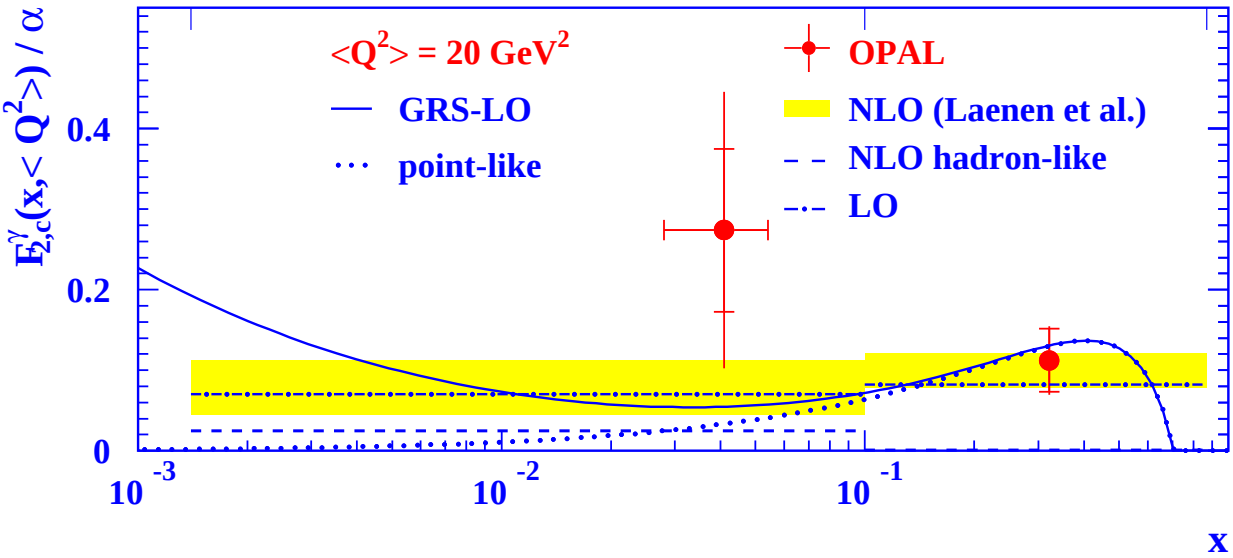

The x dependence of F_2^γ (GRV) and F_2^γ (asy)

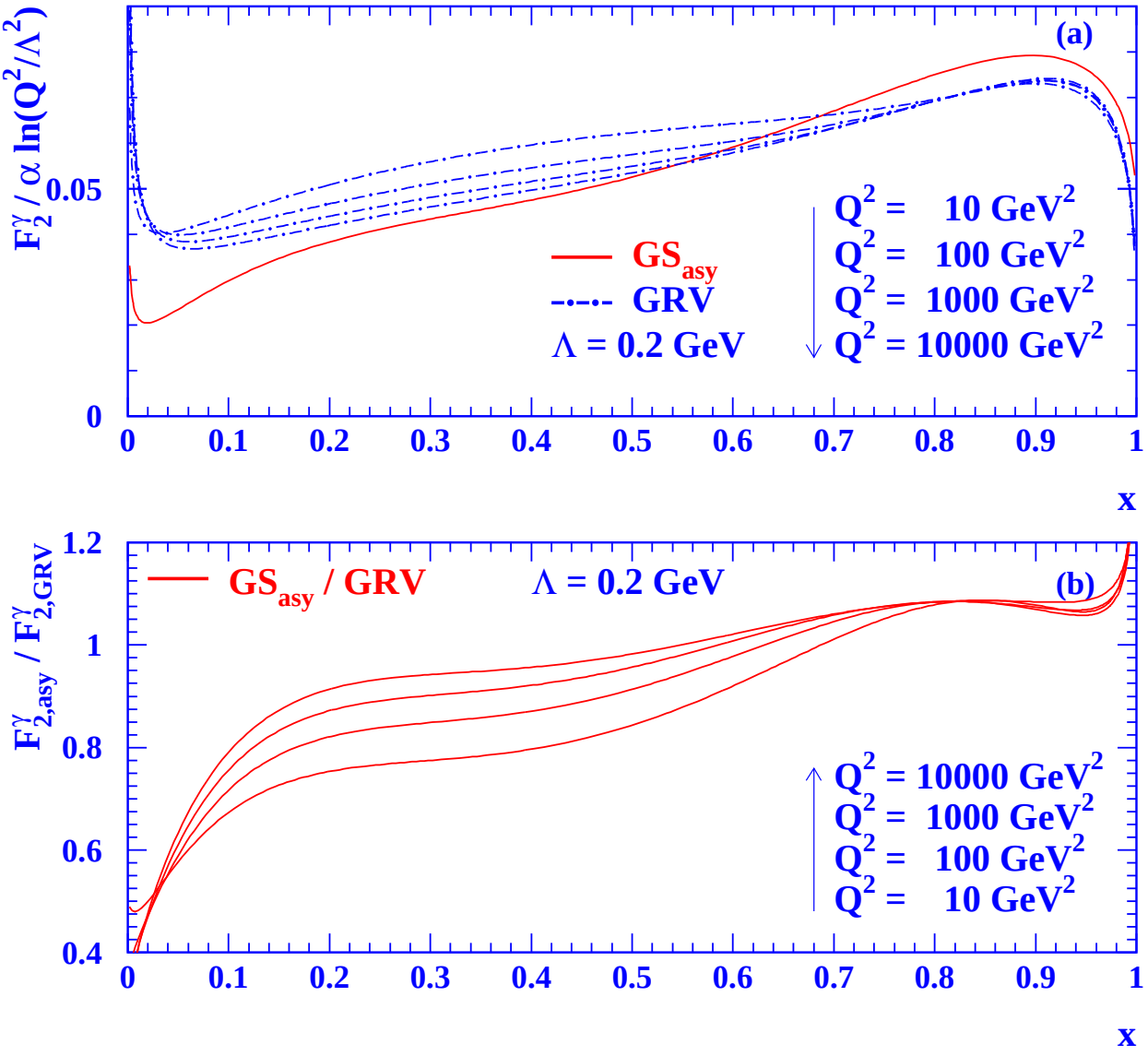

The asymptotic solution approaches the full F_2^γ at large x and Q^2.

The Q^2 evolution of F_2^γ for $n_f = 3$

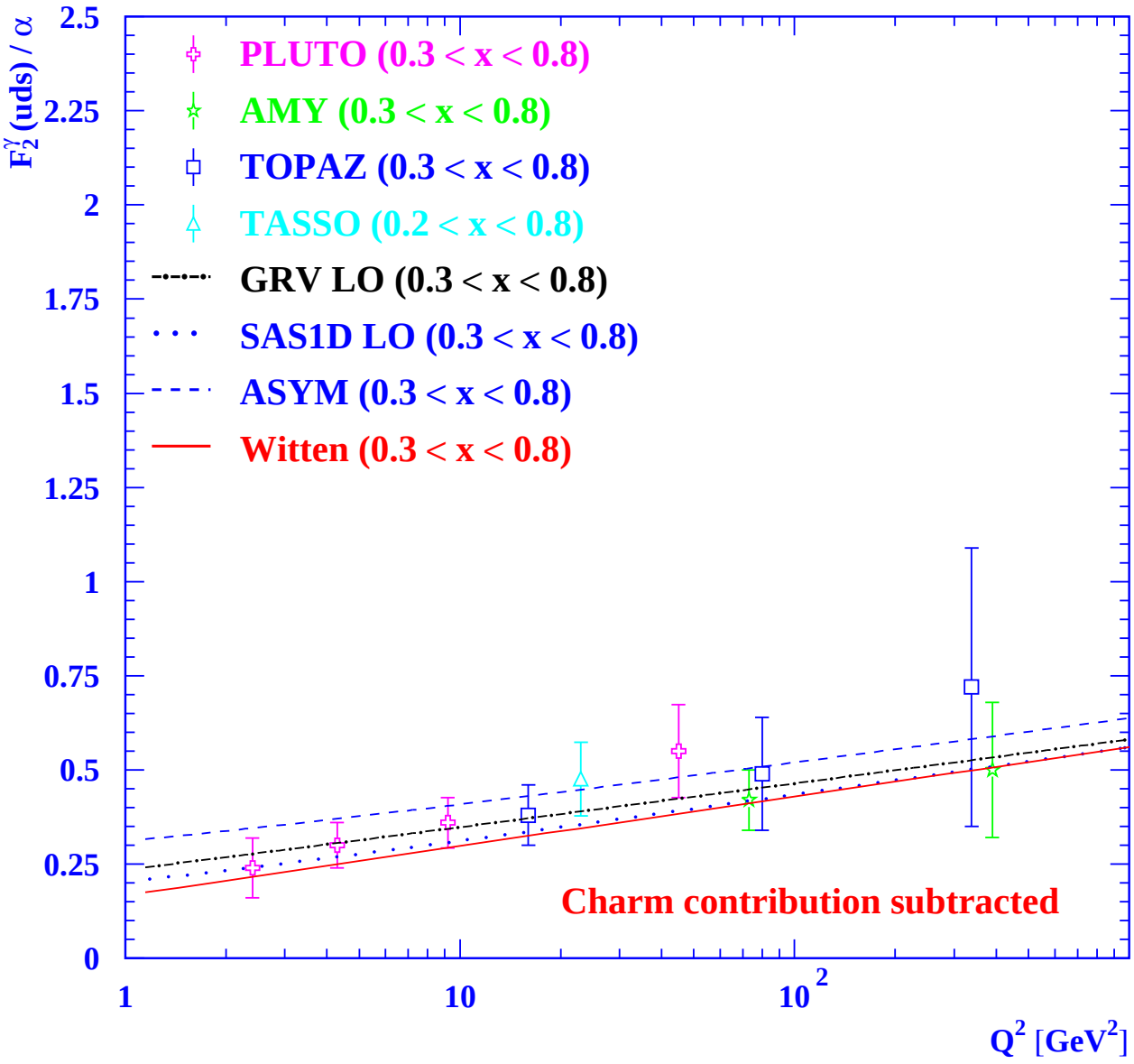

A clear rise consistent with $\ln Q^2$ is seen in the data.

All predictions are consistent with the data.

The Q^2 evolution of F_2^γ for $n_f = 4$

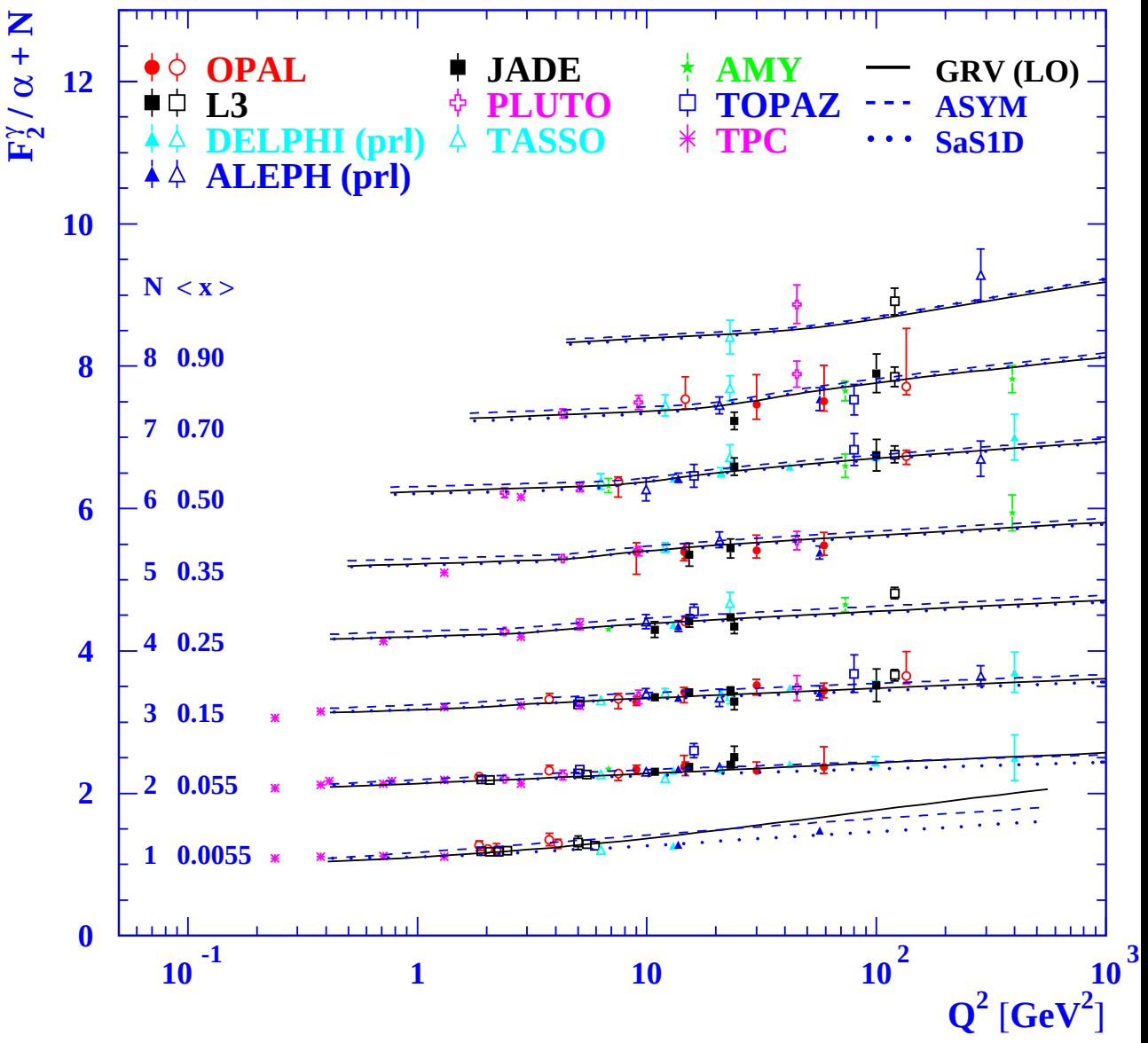

The slope increases with increasing x

The Q^2 evolution of F_2^γ compared to linear fits

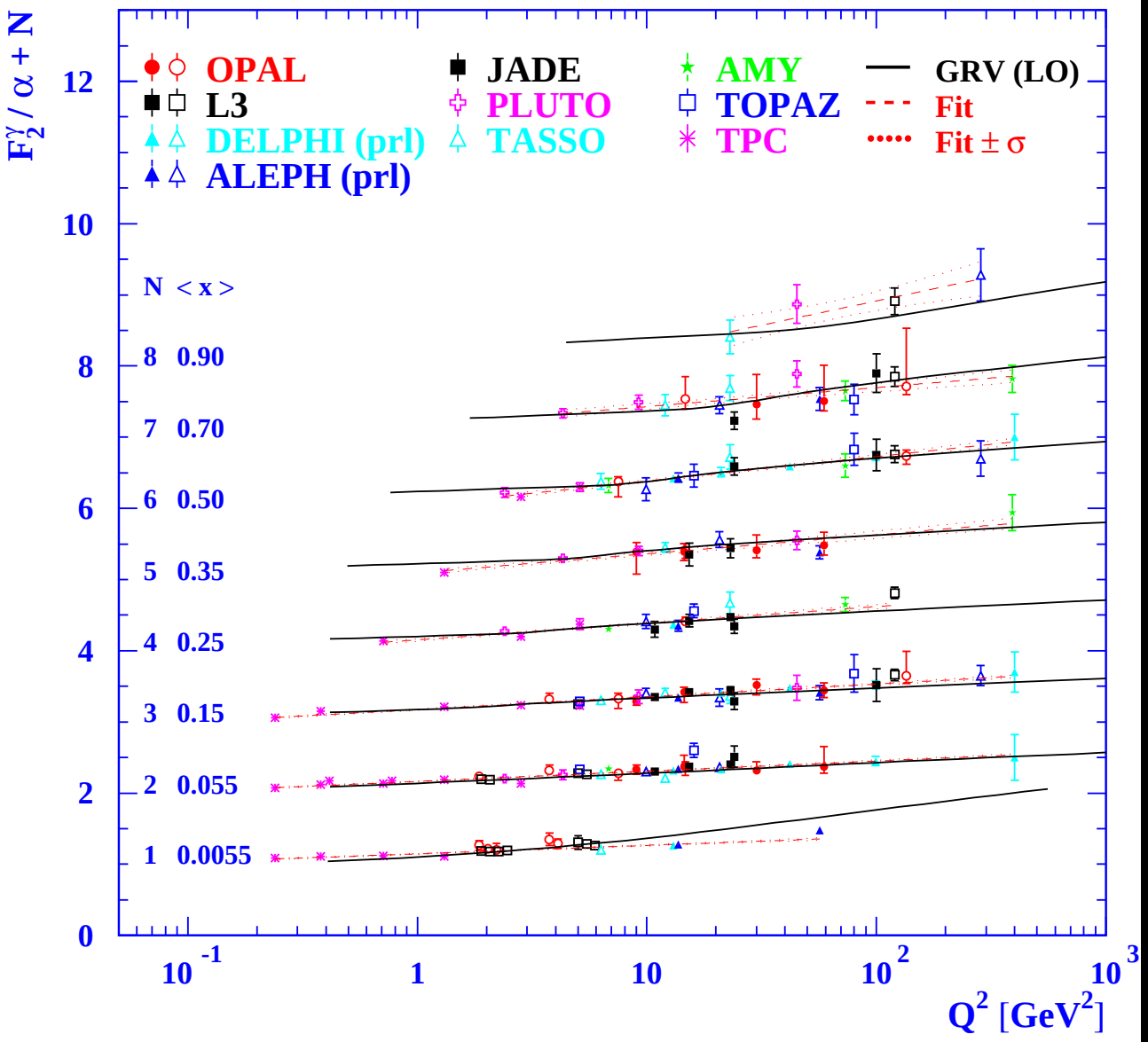

At present linear fits are sufficient to describe the data

The Q^2 evolution of F_2^γ after charm subtraction

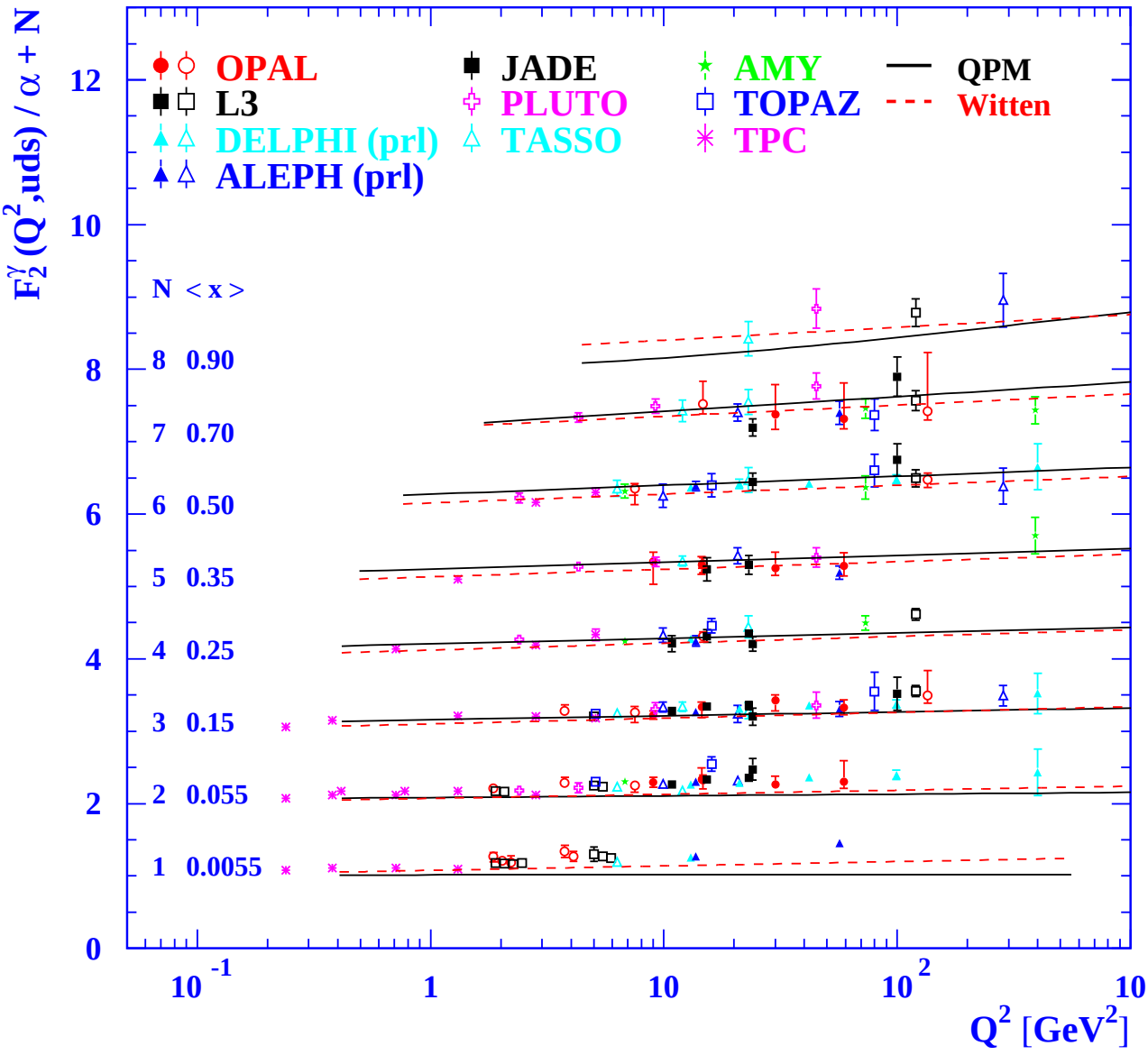

The asymptotic prediction from Witten is closer to the data than the QPM prediction.

The future of the F_2^γ measurements

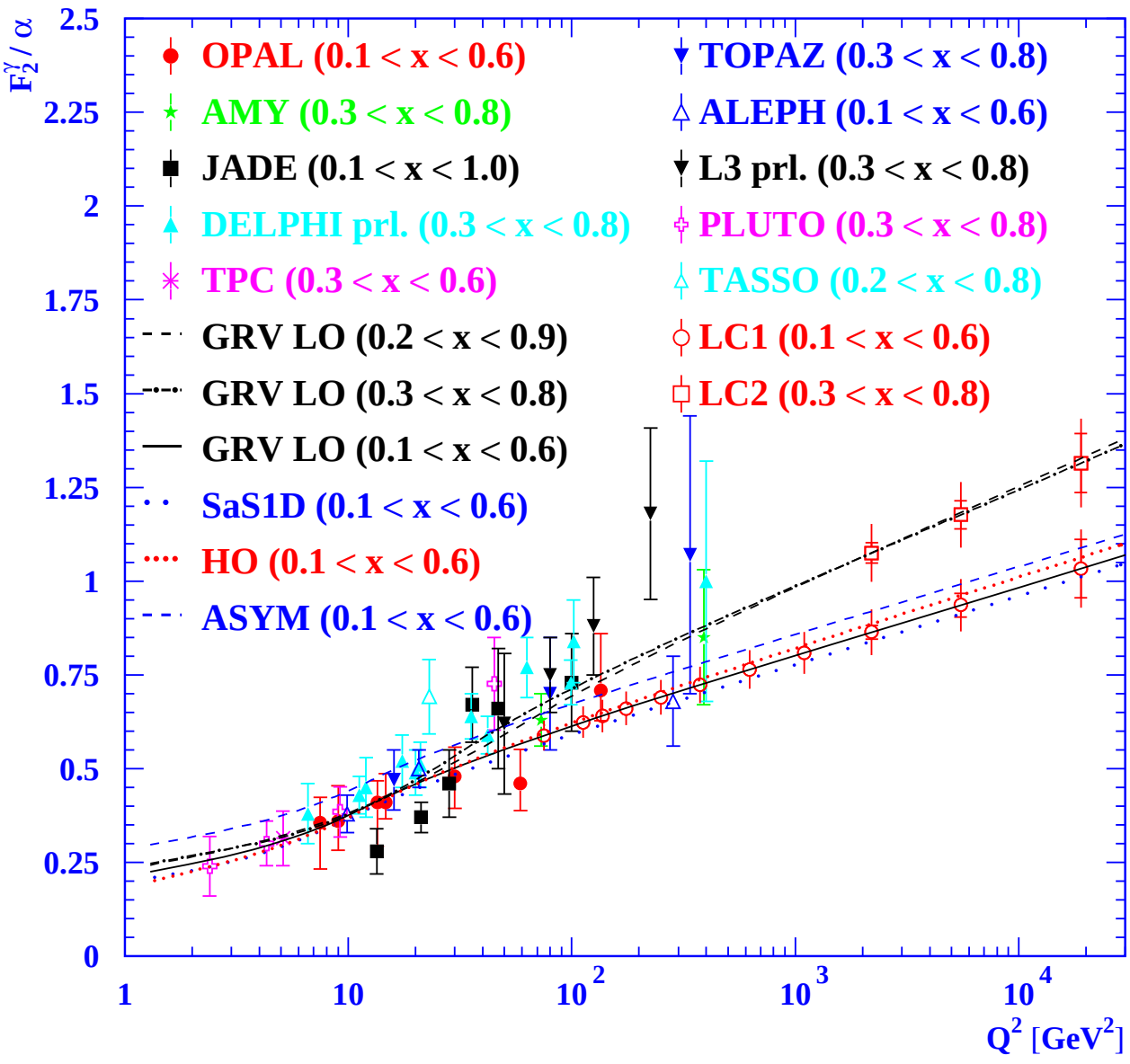

The Linear Collider (LC) will play an important role in testing this fundamental prediction of perturbative QCD.

F_2^γ for virtual photons

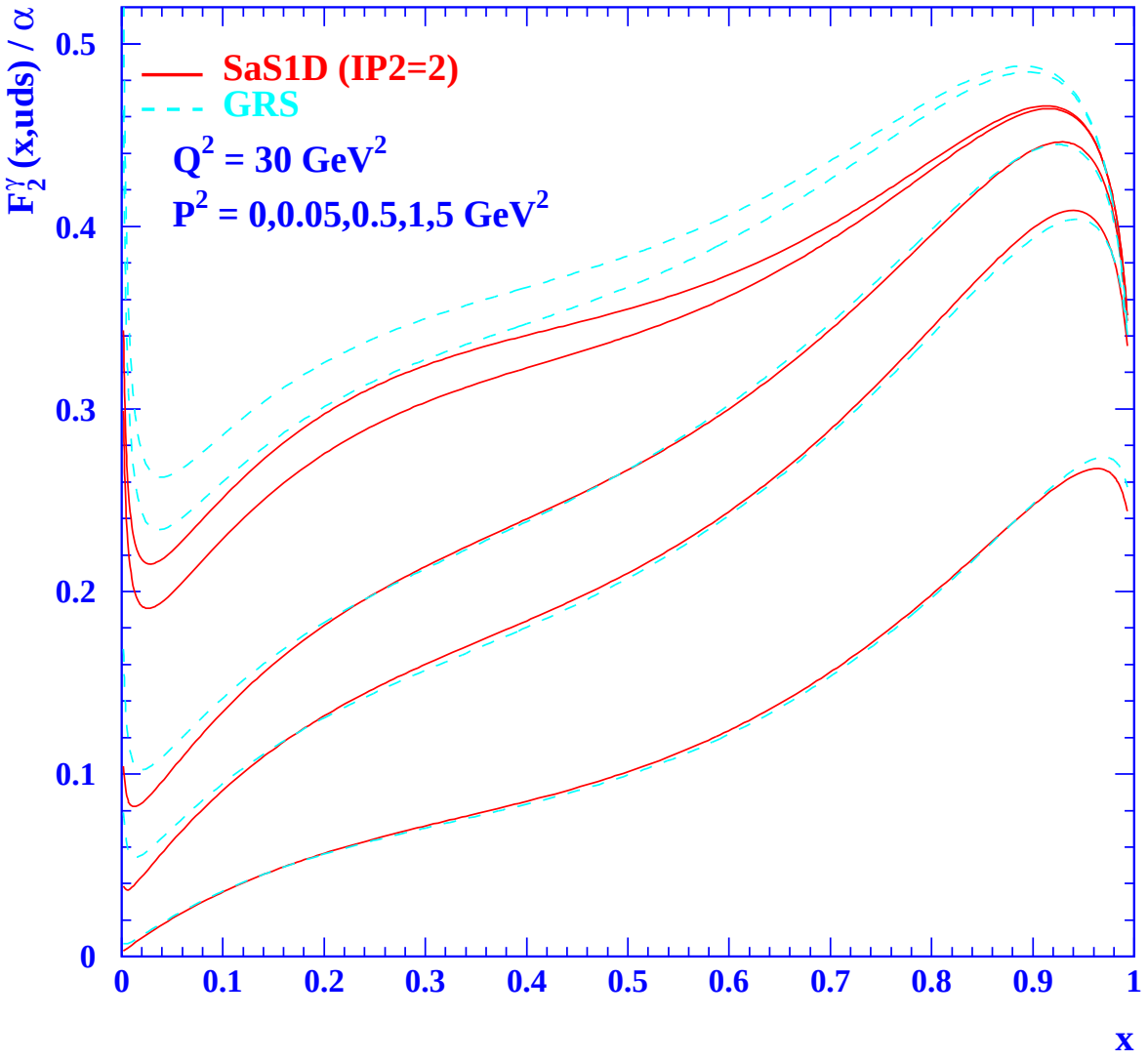

The absolute predictions agree for $P^2 > 0.5\ \mathrm{GeV}^2$, when using SaS1D ($IP2 = 2$)

The x dependence of $F_2^\gamma\ (P^2)$(GRS) and $F_2^\gamma\ (P^2)$(pl)

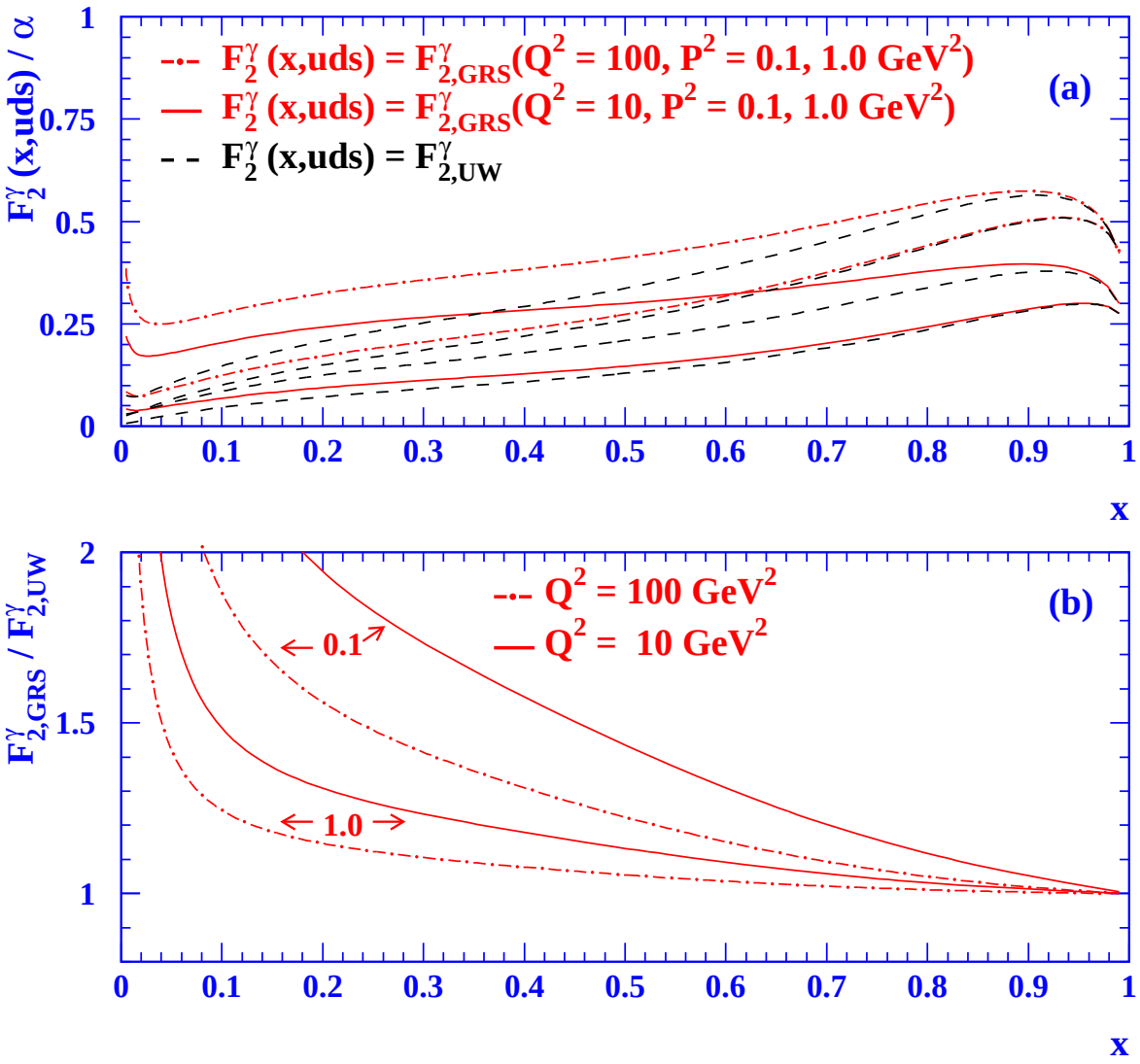

The non perturbative part is a 10% correction for $x > 0.3, Q^2 = 100\ \mathrm{GeV}^2$ and $P^2 = 1\ \mathrm{GeV}^2$

The Measurement of $F_{\mathrm{eff}}^{\gamma}$ from PLUTO

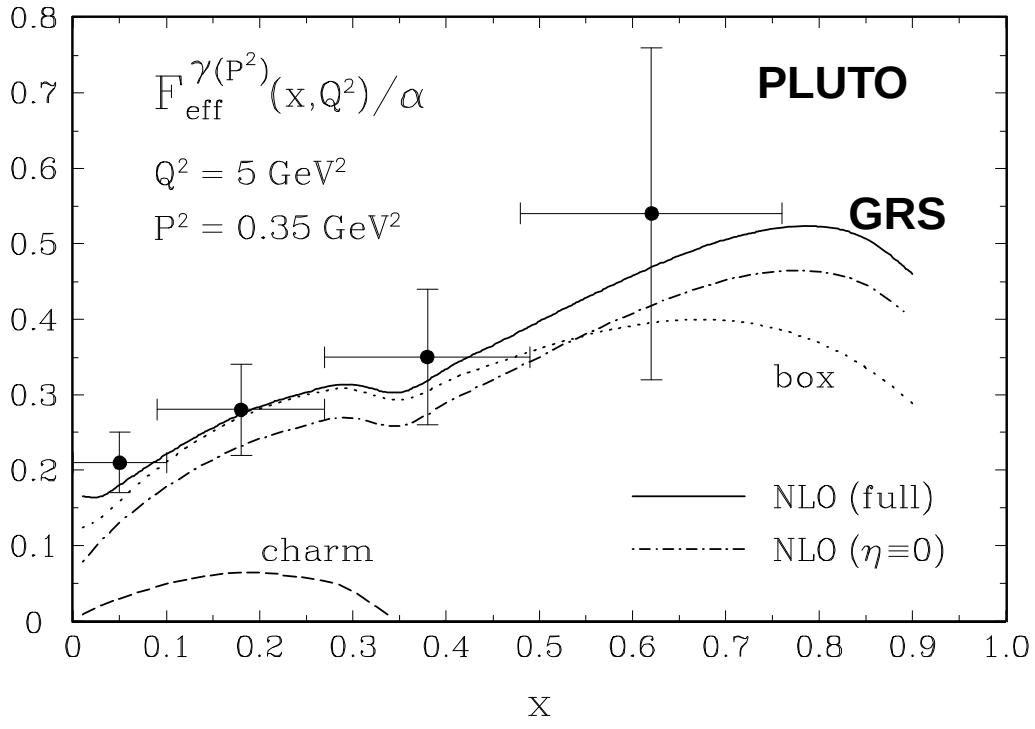

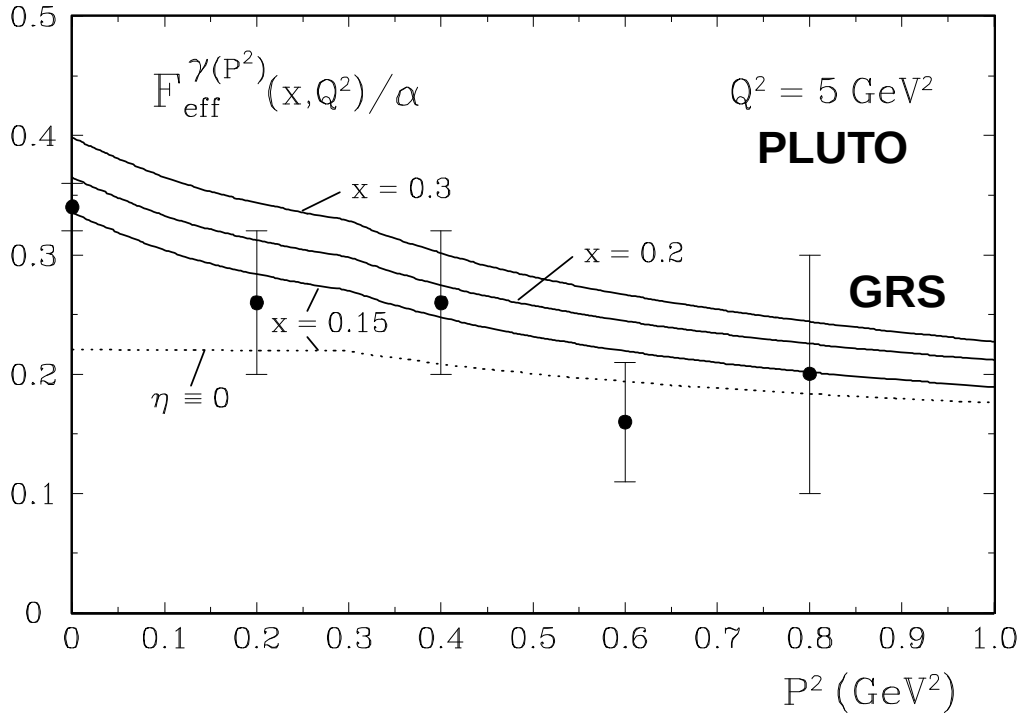

F_2^γ and $F_{\rm eff}^\gamma$ from L3

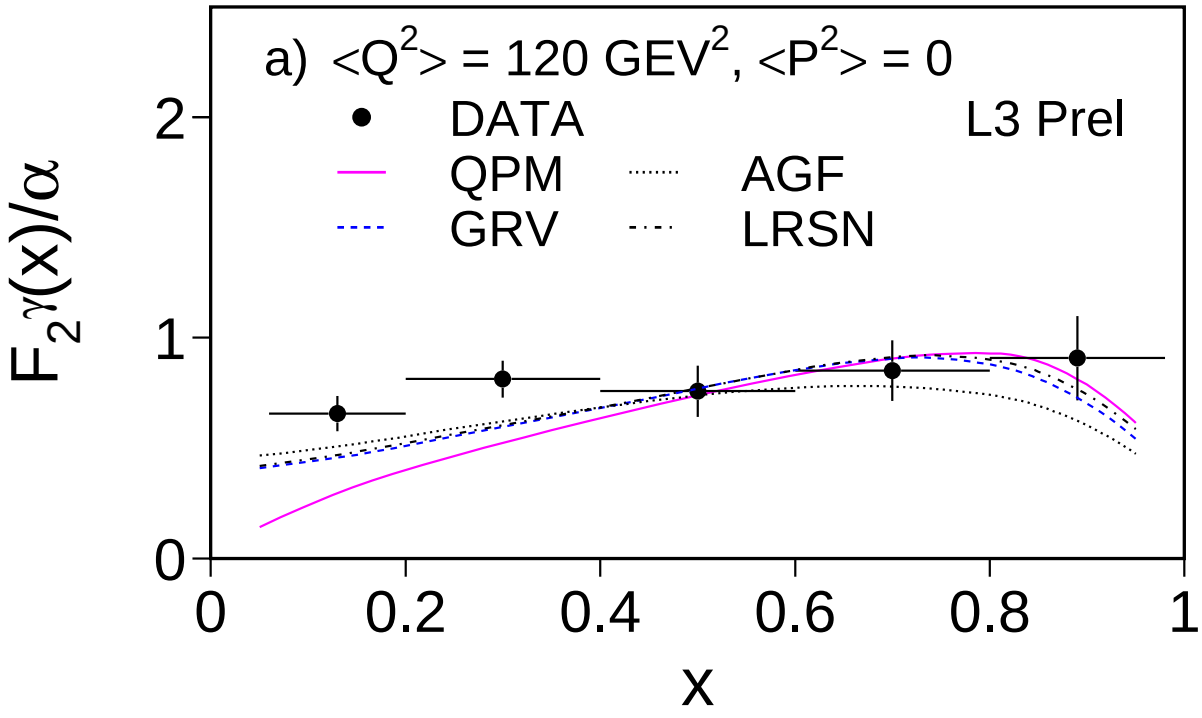

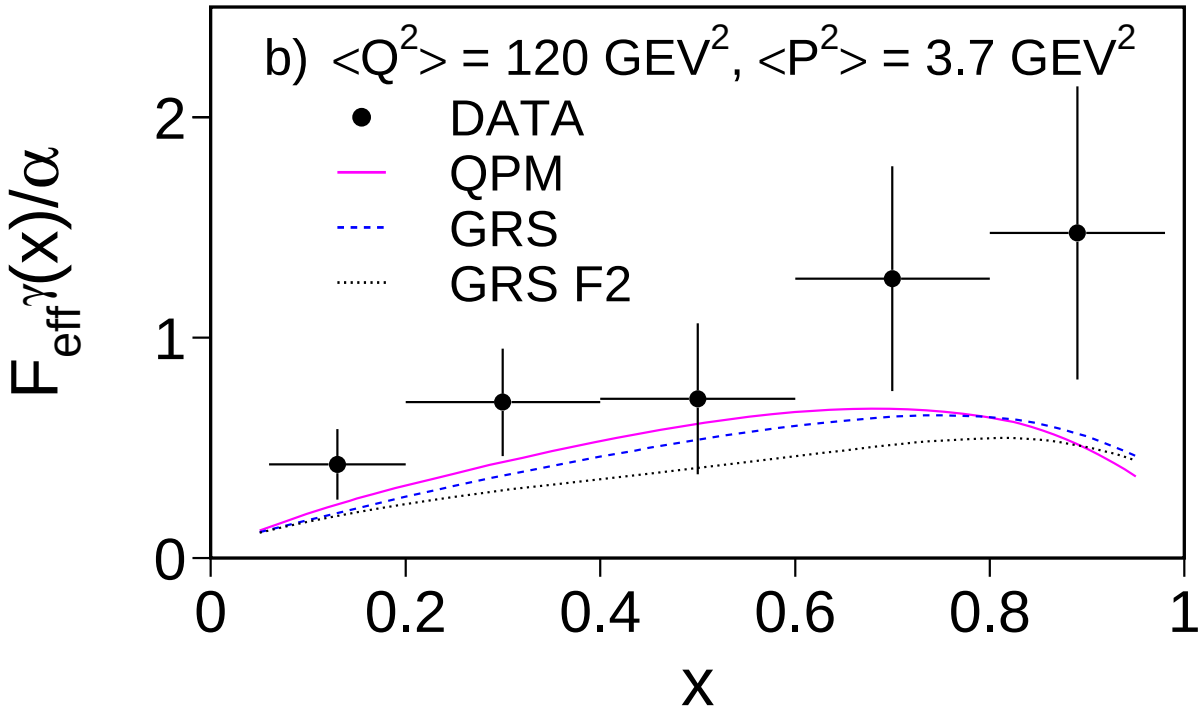

The cross-section for double tags

for $ee \rightarrow ee\gamma^{\star}\gamma \rightarrow ee\mu^{+}\mu^{-}$

OPAL

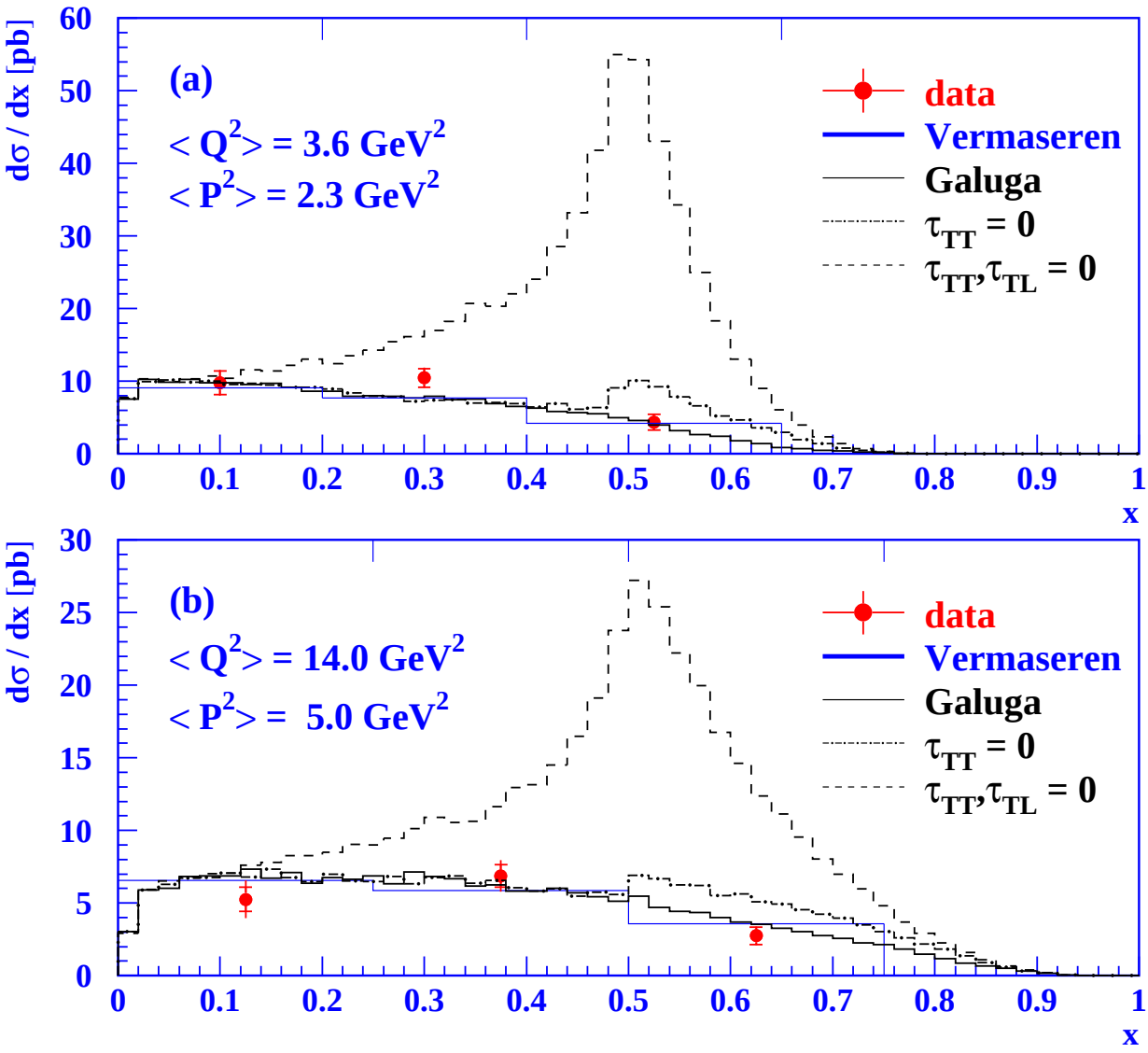

QED agrees well with the data and the presence of the interference terms is clearly seen for the first time.

Cross-section for $ee \rightarrow ee$ hadrons

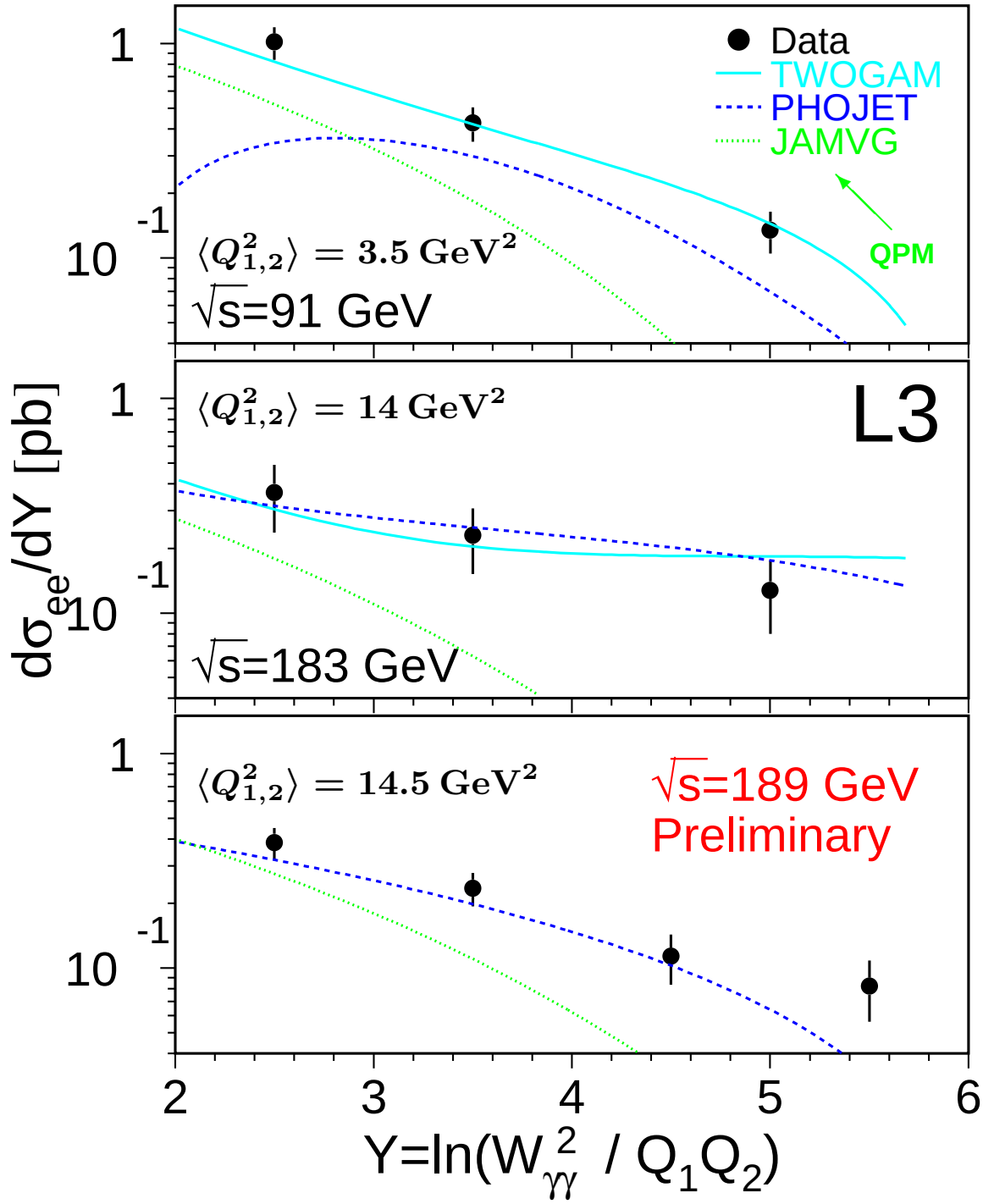

Differential cross-sections

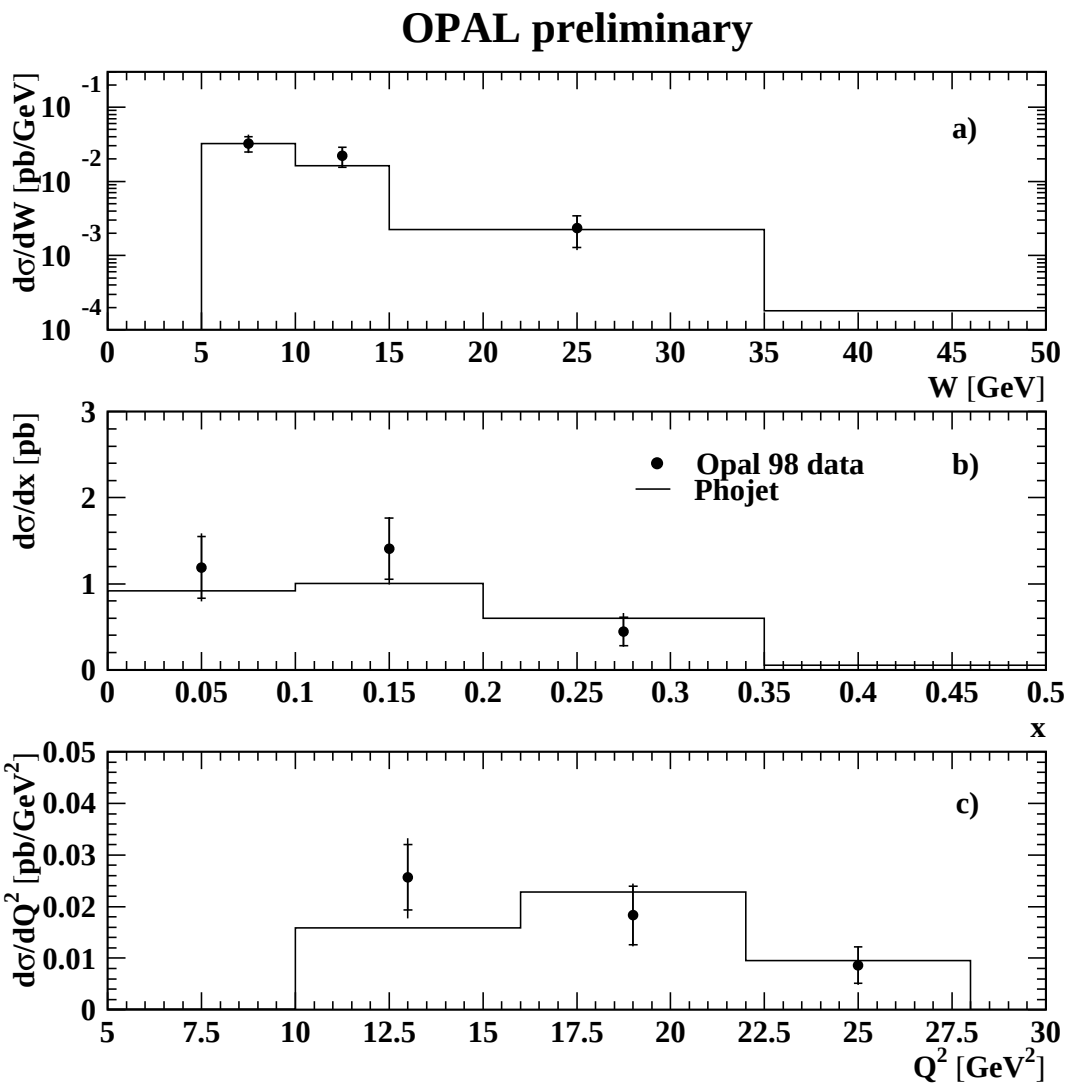

Cross-section corrected to:

$E_e > E, 34 < \theta_e < 55$ mrad and $W > 5$ GeV

Cross-section integrated for $2 < Y < 6$ in [pb]				
E	OPAL preliminary	Phojet	2-gluon	BFKL LO / HO
65	$0.15 \pm 0.05 \,^{+0.03}_{-0.02}$	0.17	0.14	2.2 / 0.26
33	$0.21 \pm 0.06 \,^{+0.04}_{-0.02}$	0.25	0.24	5.7 / 0.50

Leading order diagrams

Direct:

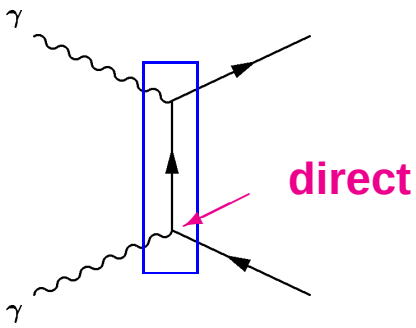

hard interaction

resolved

Single-Resolved:

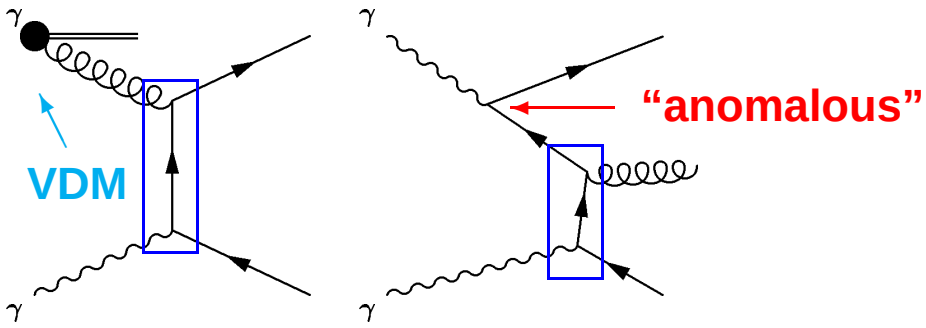

Double-Resolved:

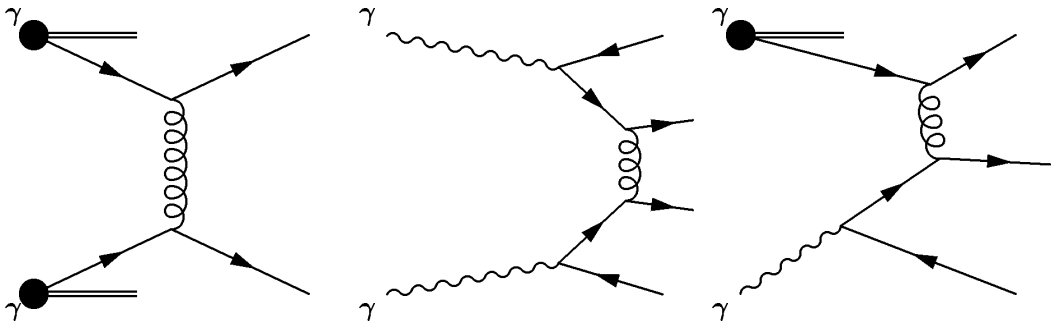

Monte Carlo models

PYTHIA and PHOJET

Monte Carlo ingredients:

1. Leading order (LO) QCD matrix elements
2. Hard and soft processes
3. Total cross sections from Regge models
4. Initial state parton radiation
5. Fragmentation based on JETSET
6. Multiple interactions

NLO calculations

- NLO particle spectra by J. Binnewies, B.A. Kniehl and G. Kramer
- NLO jet cross-sections by M. Klasen, T. Kleinwort and G. Kramer

Comparison to γp, hp data and to a NLO calculation

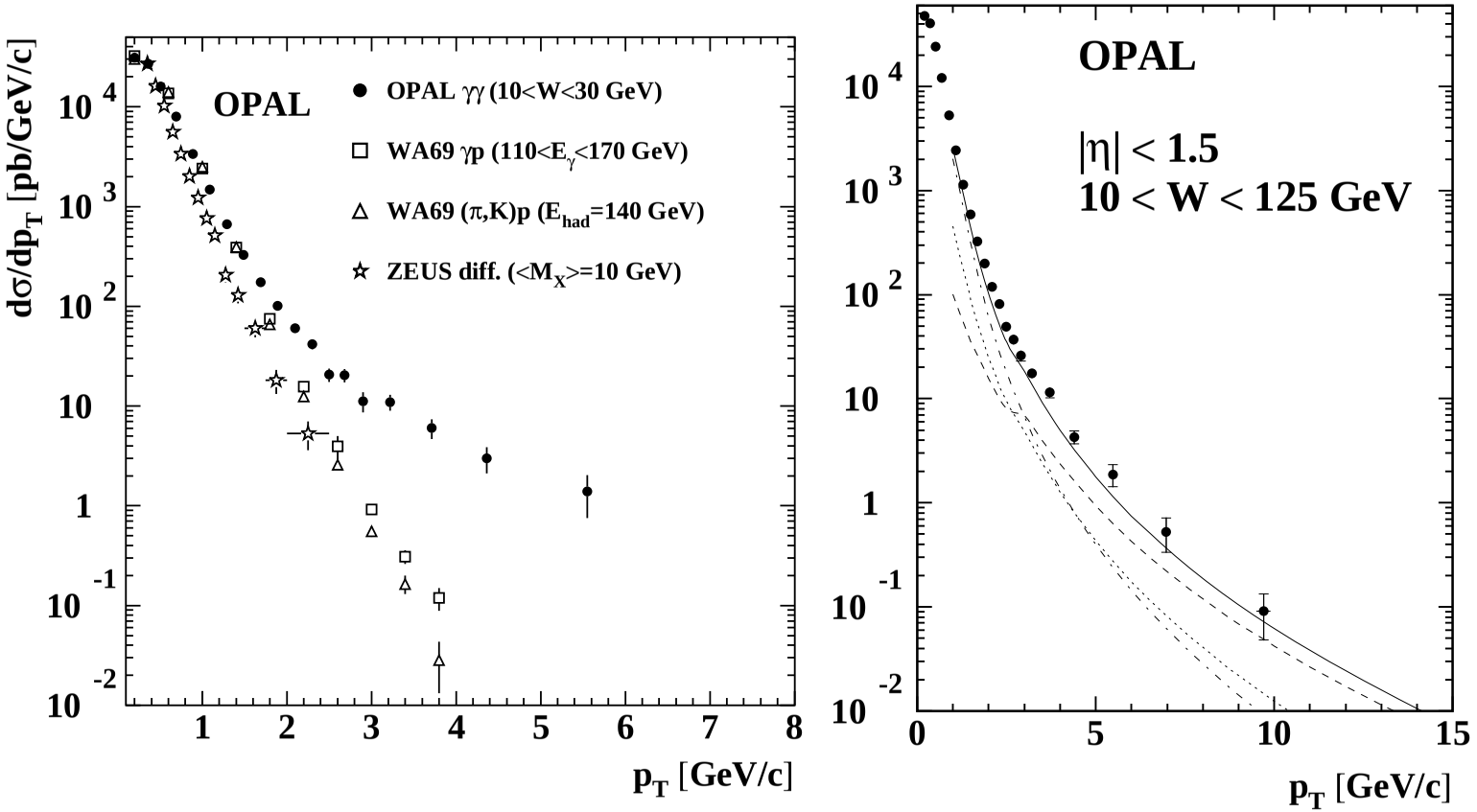

The hard component due to the pointlike coupling of the photon is clearly seen in the data. The NLO calculation gives a fair description of the data.

The angular dependencies of different processes

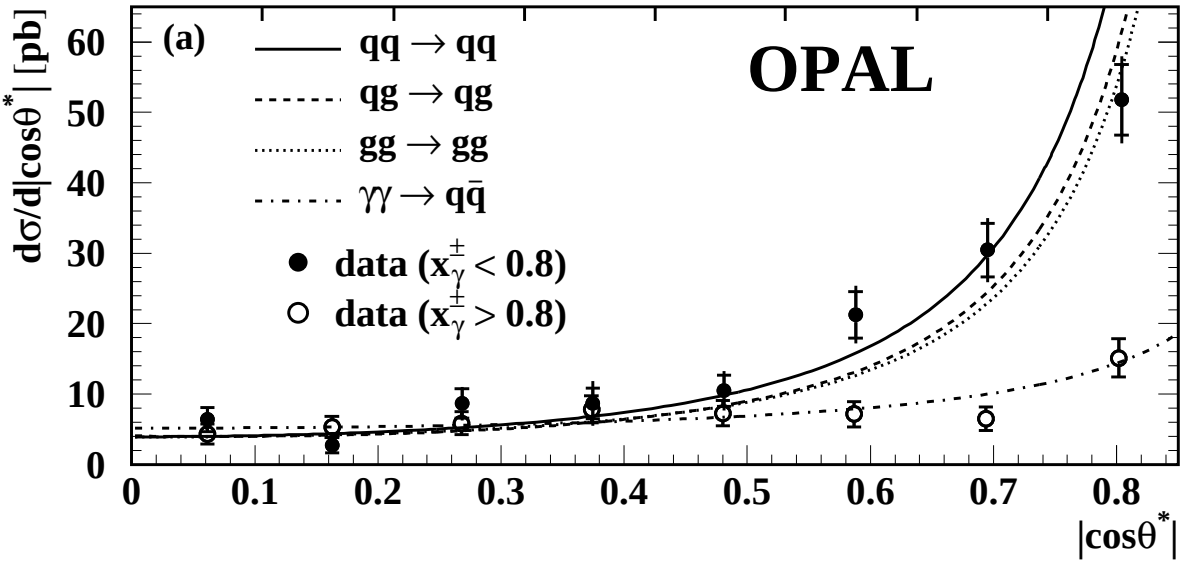

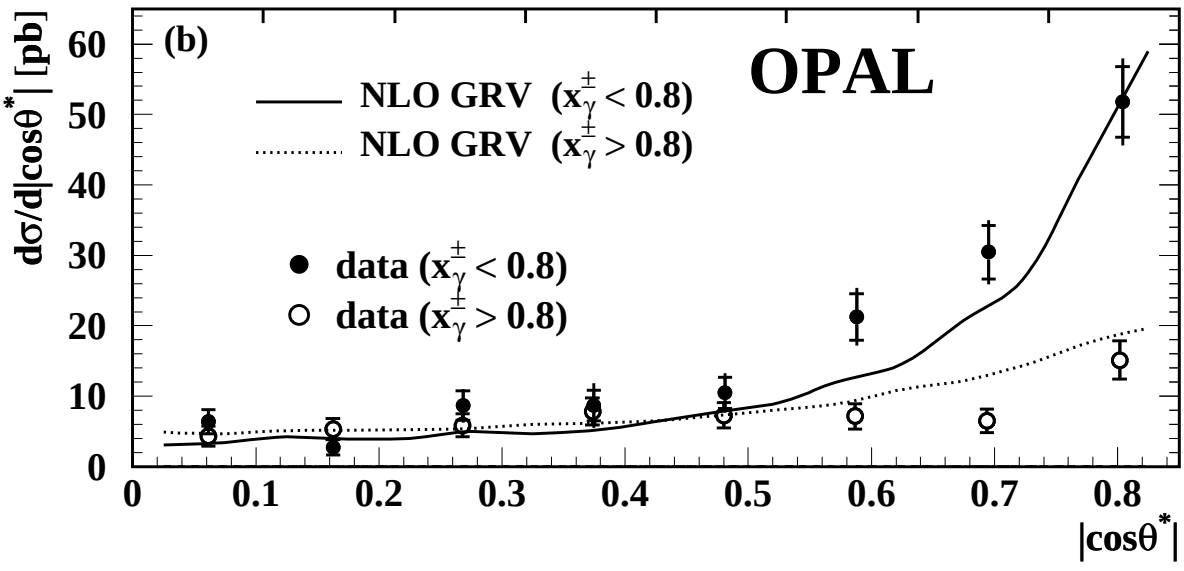

The angular dependencies of the different processes can be clearly disentangled

Differential di-jet cross-section as a function of E_T

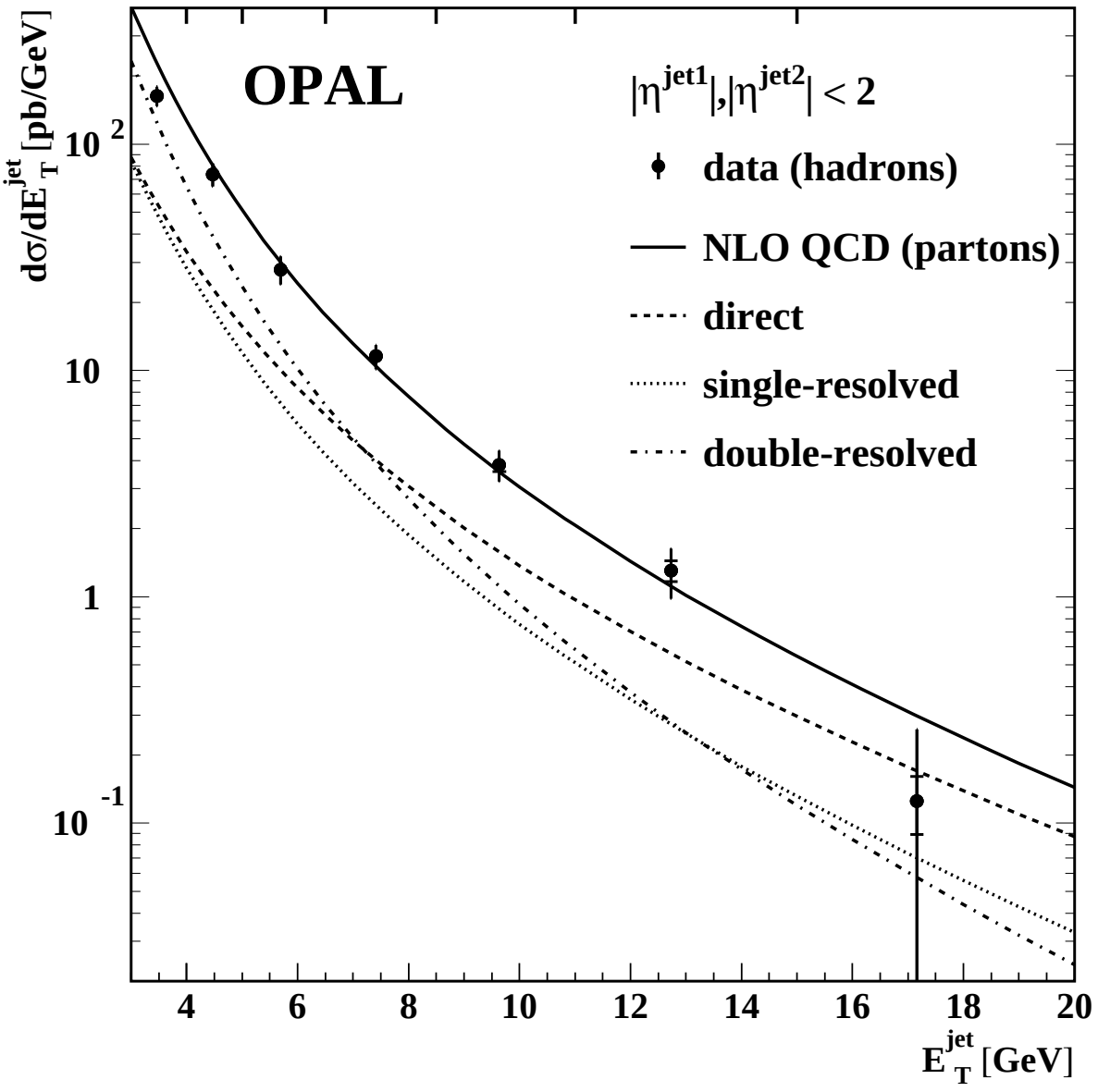

The NLO calculation is in fair agreement with the data

The W distributions for anti-tagged events

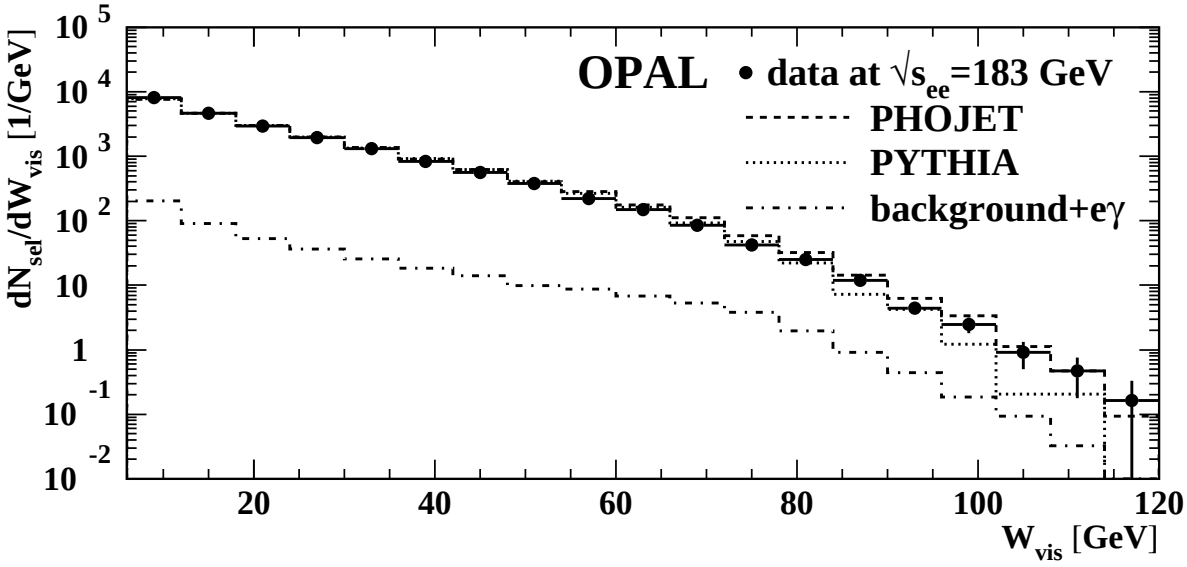

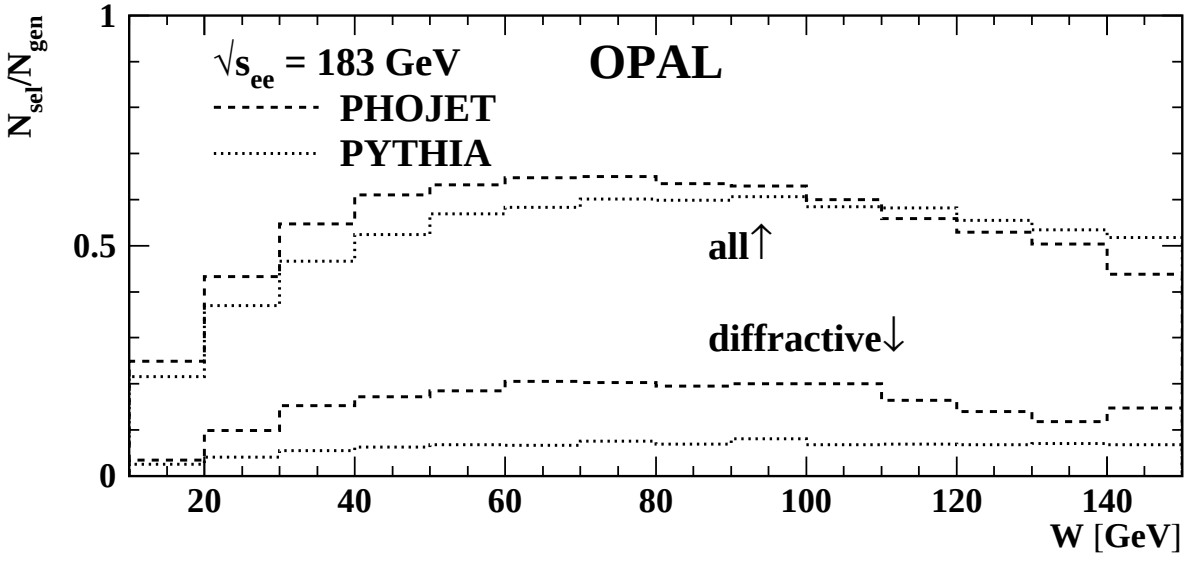

The acceptance for diffractive and elastic events is very different for the Phojet and Pythia models

The total hadronic cross-section at various $\sqrt{s_{ee}}$

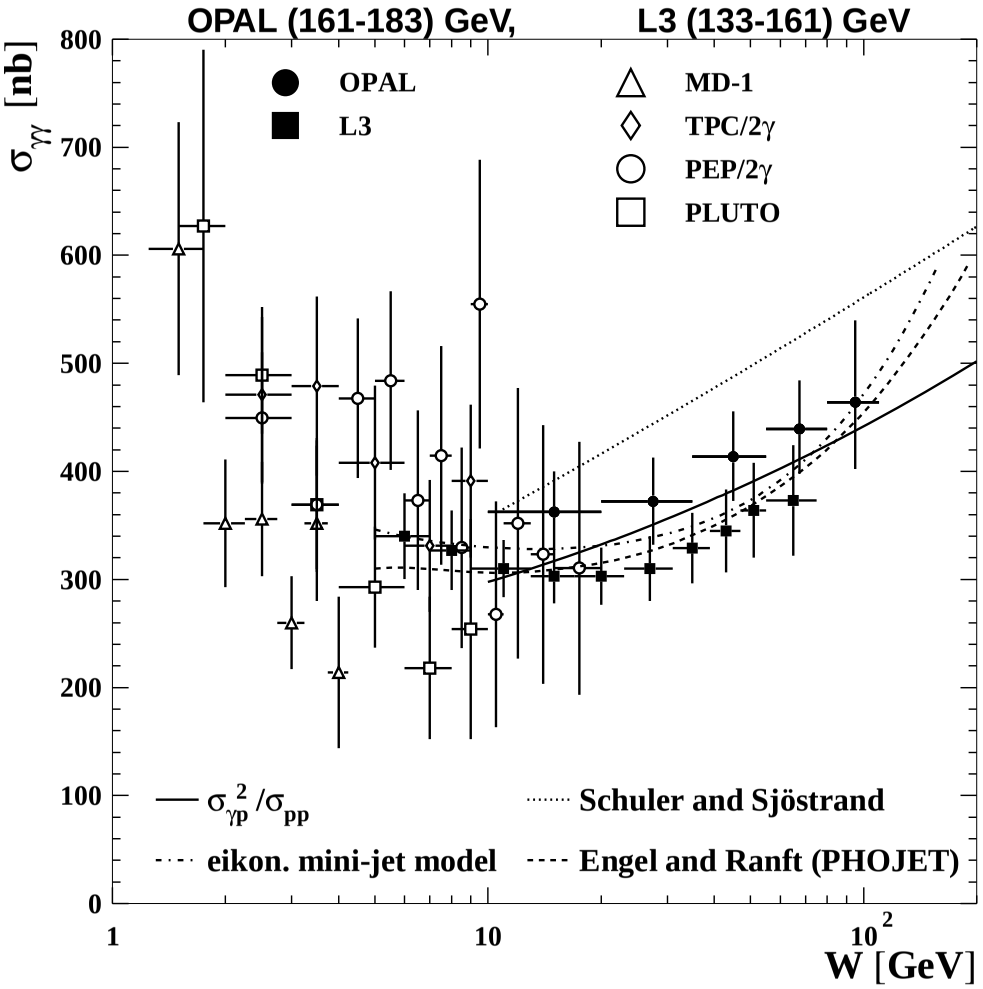

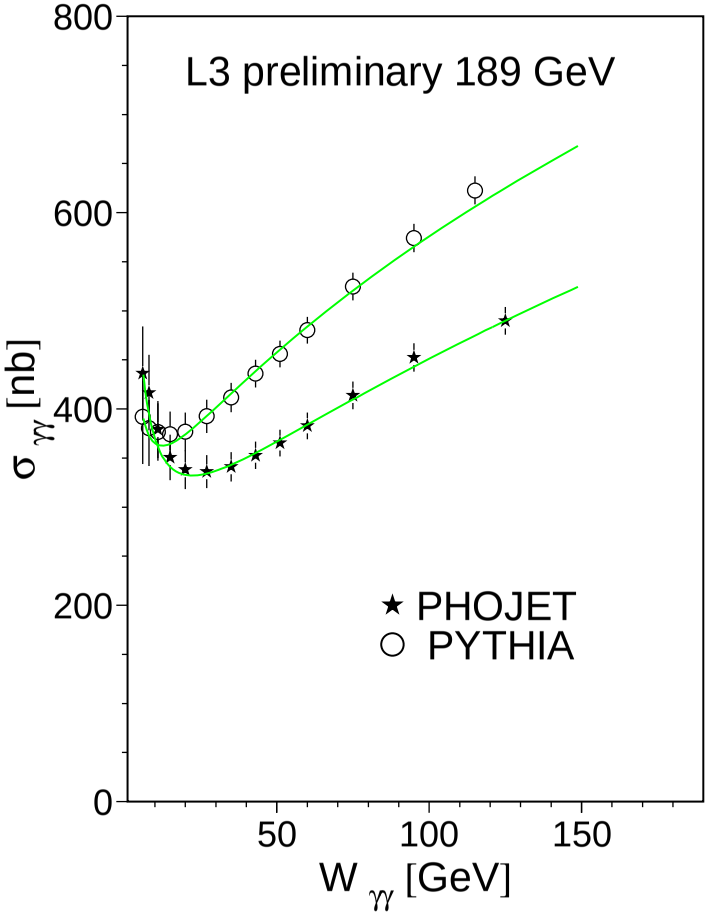

A clear rise of the total cross-section is observed in the data

The various fits to $\sigma_{\gamma\gamma}$

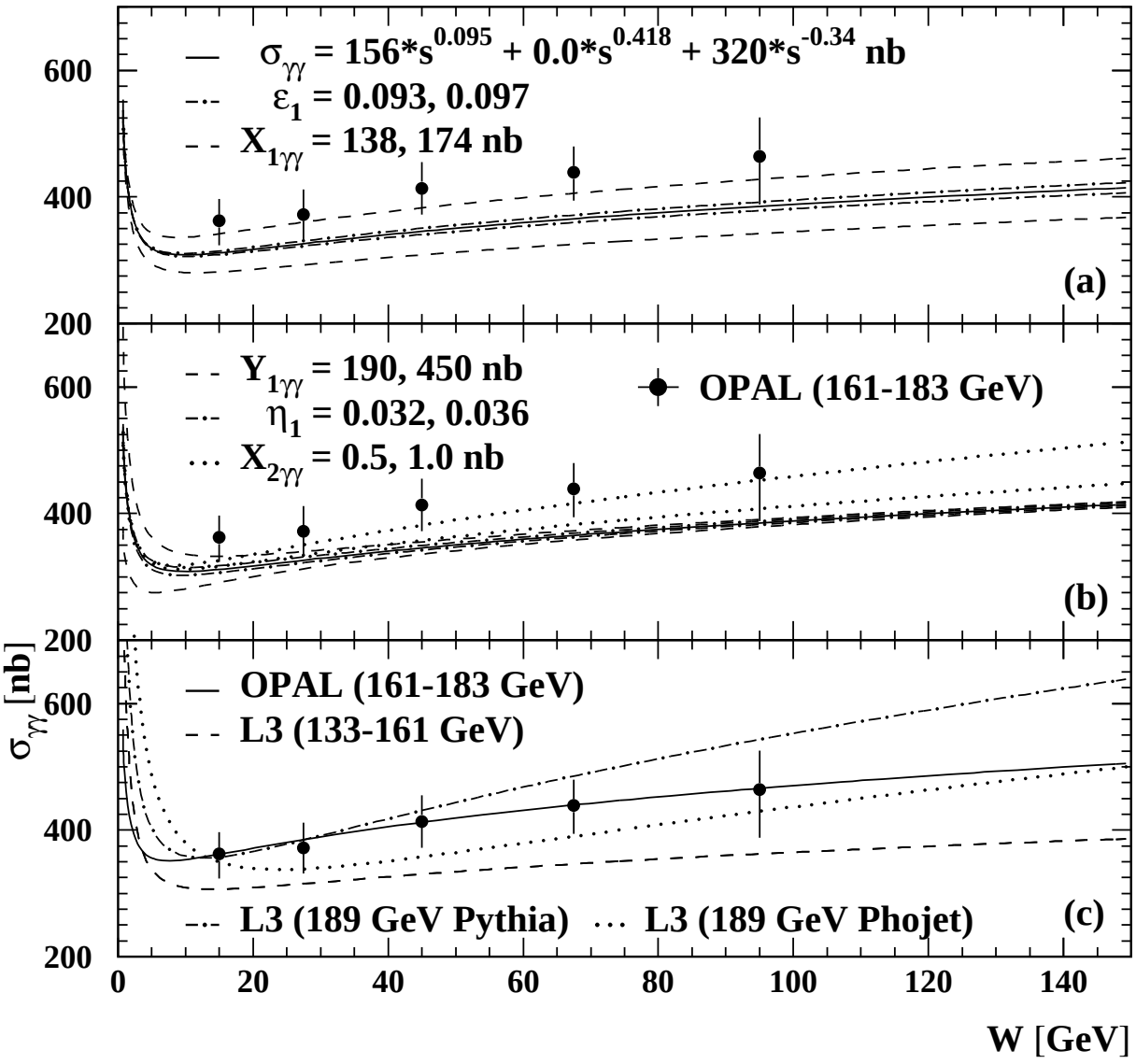

A clear rise of the total cross-section is observed in the data. The size of the rise, however, is unclear at the moment.

Inclusive charm production

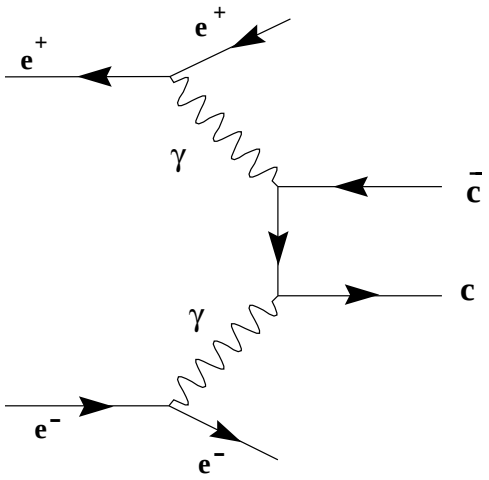

Direct

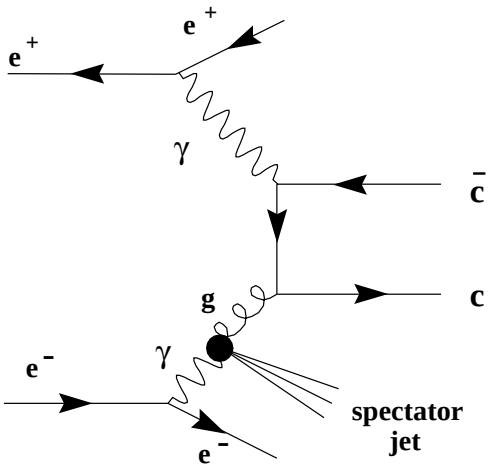

Single Resolved

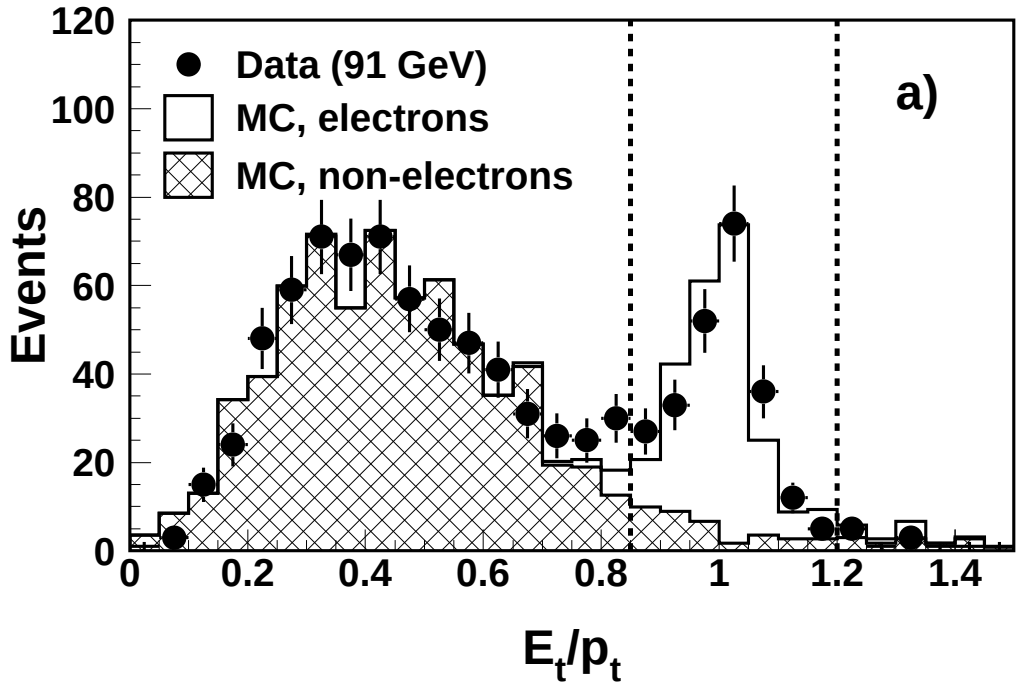

A clear electron signal of the semileptonic charm decays is observed

The differential D* cross-section

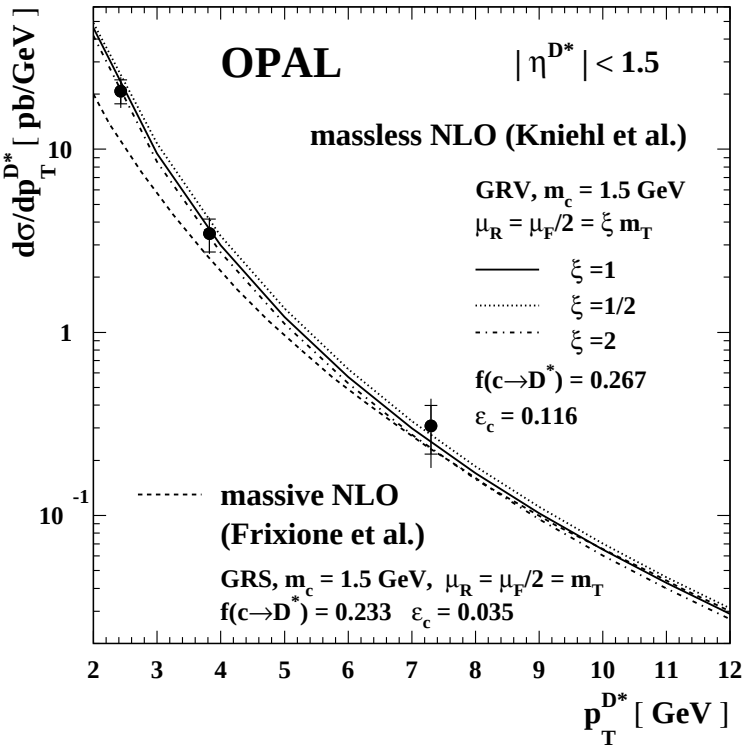

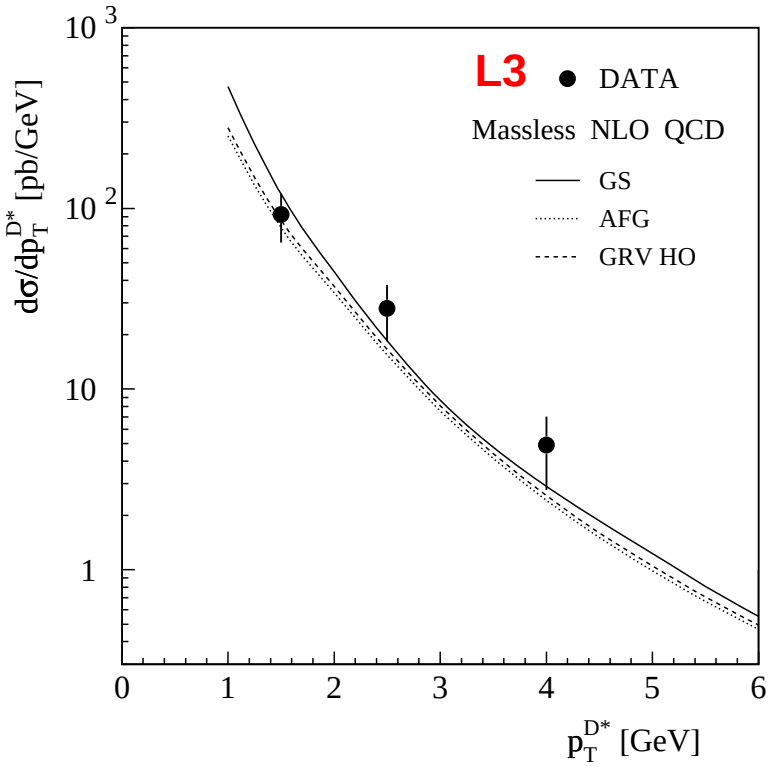

The NLO QCD calculation agrees well with the data.

The inclusive charm cross-section

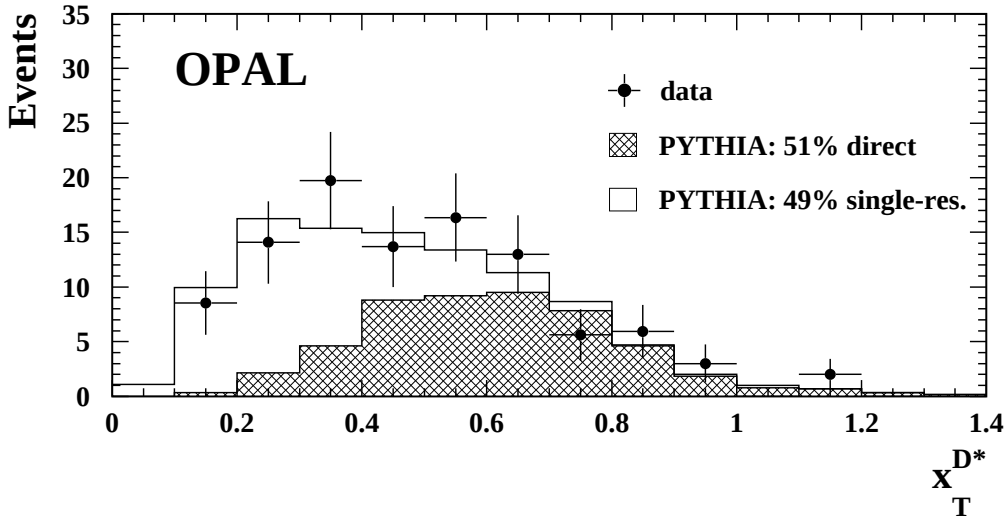

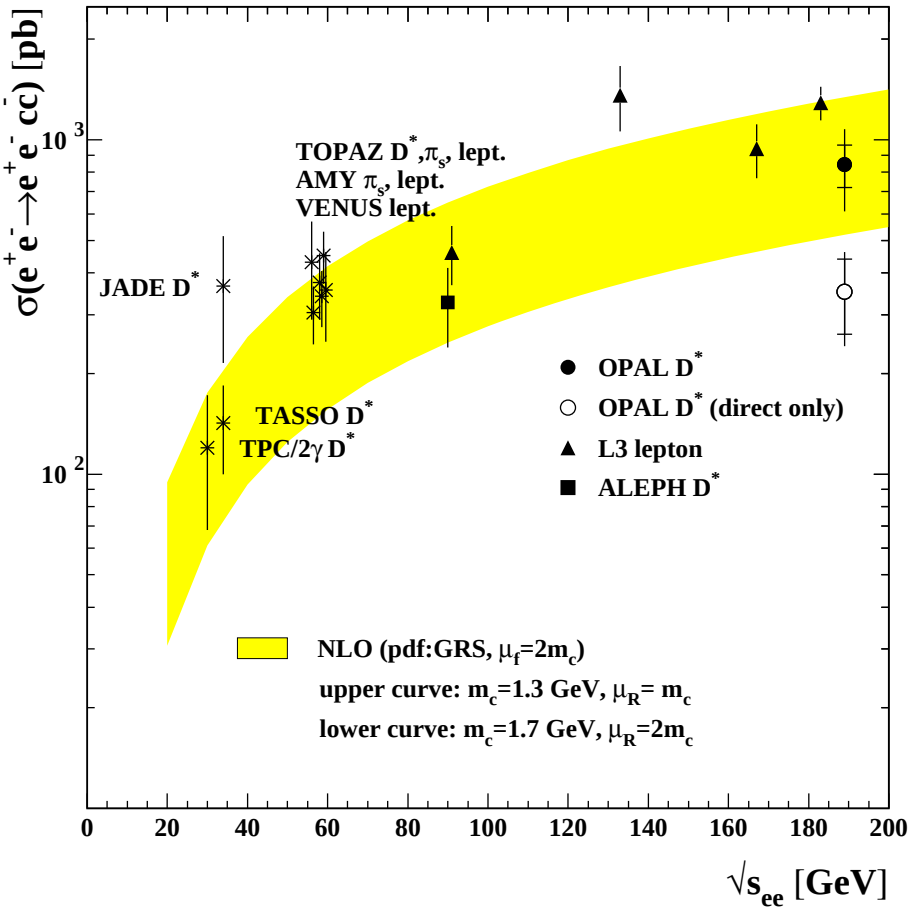

The direct charm production alone is insufficient to describe the data

Search for Bottom production

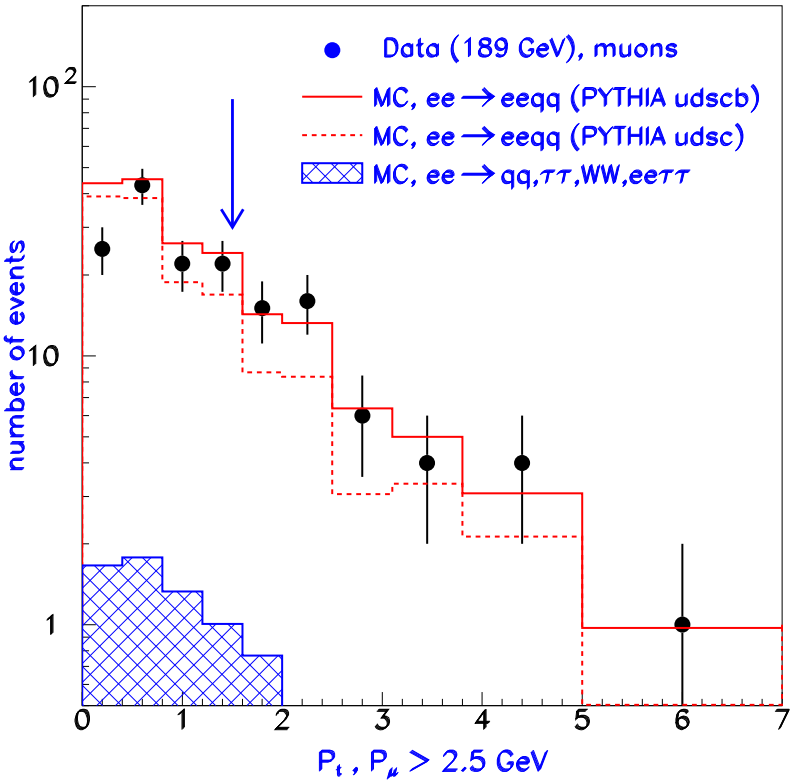

$p_t^\mu > 1.5$ GeV

$N_{ev}^\mu = 49$

$\epsilon_b^\mu = 0.9\%$

$\Pi_b^\mu = 34\%$

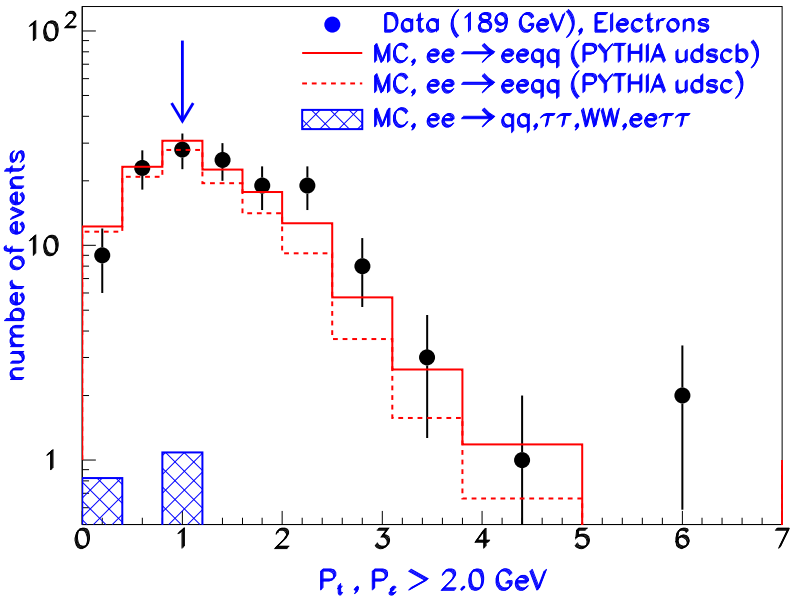

$p_t^e > 1.0$ GeV

$N_{ev}^e = 96$

$\epsilon_b^e = 1.6\%$

$\Pi_b^e = 28\%$

The excess in the tail is attributed to bottom.

Heavy quark production from L3

Results for $\sqrt{s_{ee}} = 189\ \mathrm{GeV}$

$$\sigma^{\mu}_{b\bar{b}} = 10.3 \pm 4.6(\mathrm{stat}) \pm 3.3(\mathrm{sys})$$

$$\sigma^{e}_{b\bar{b}} = 9.6 \pm 3.6(\mathrm{stat}) \pm 4.1(\mathrm{sys})$$

$$\sigma_{b\bar{b}} = 9.9 \pm 2.9(\mathrm{stat}) \pm 3.8(\mathrm{sys})$$

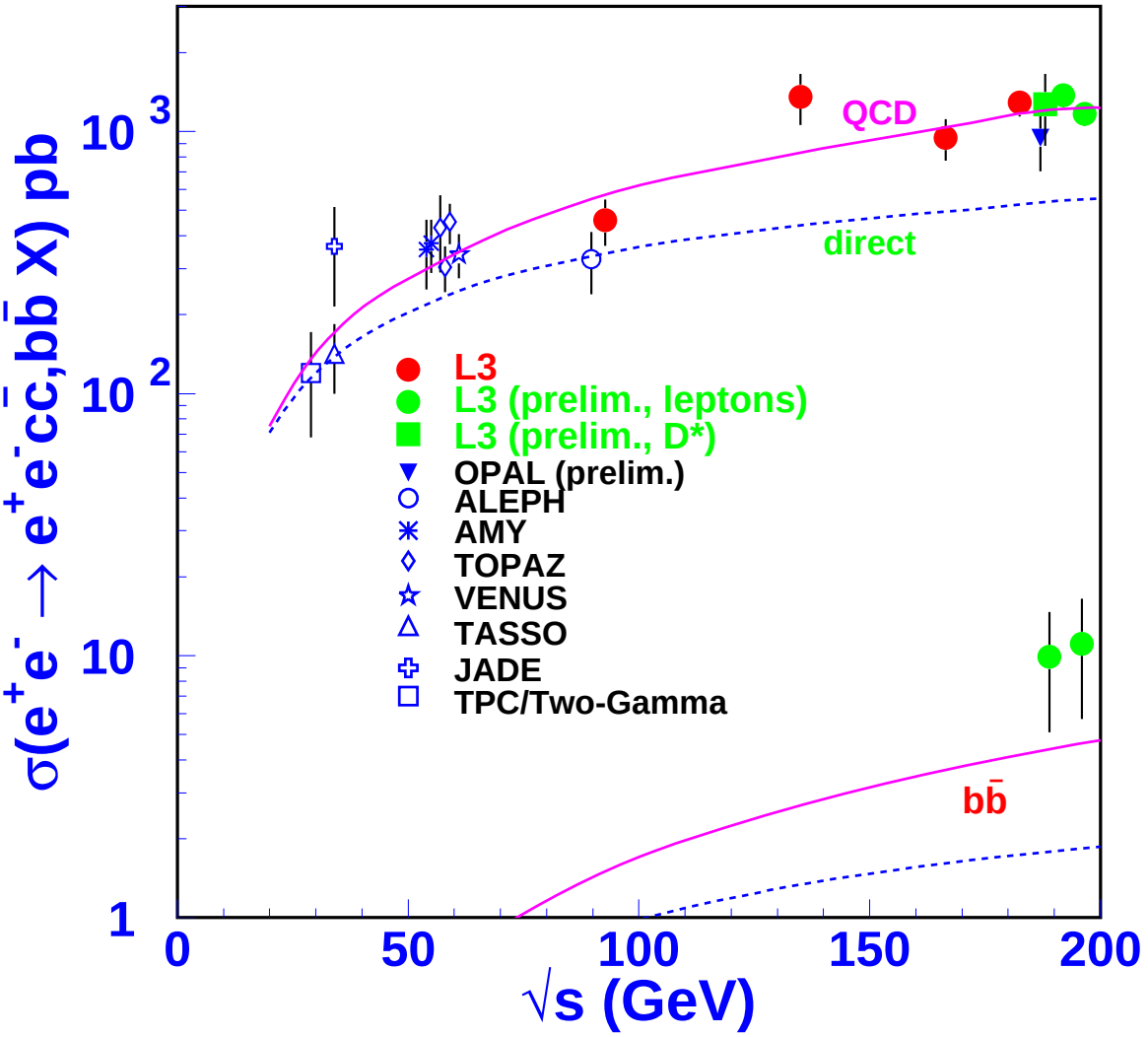

First result on bottom production in $\gamma\gamma$ scattering.

Jet production from ZEUS

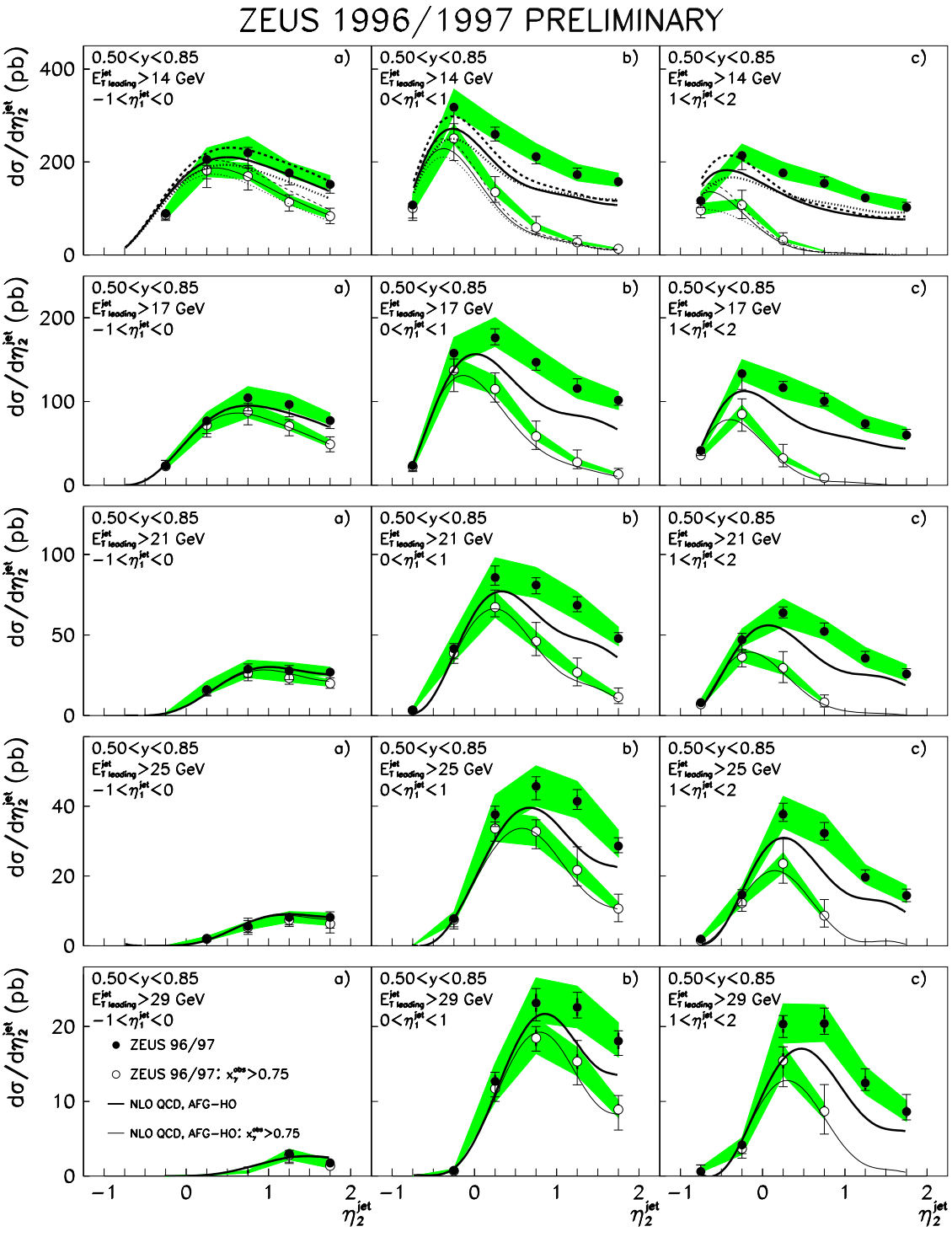

The predictions are too low at medium and large x

Structure of quasi-real photons from H1

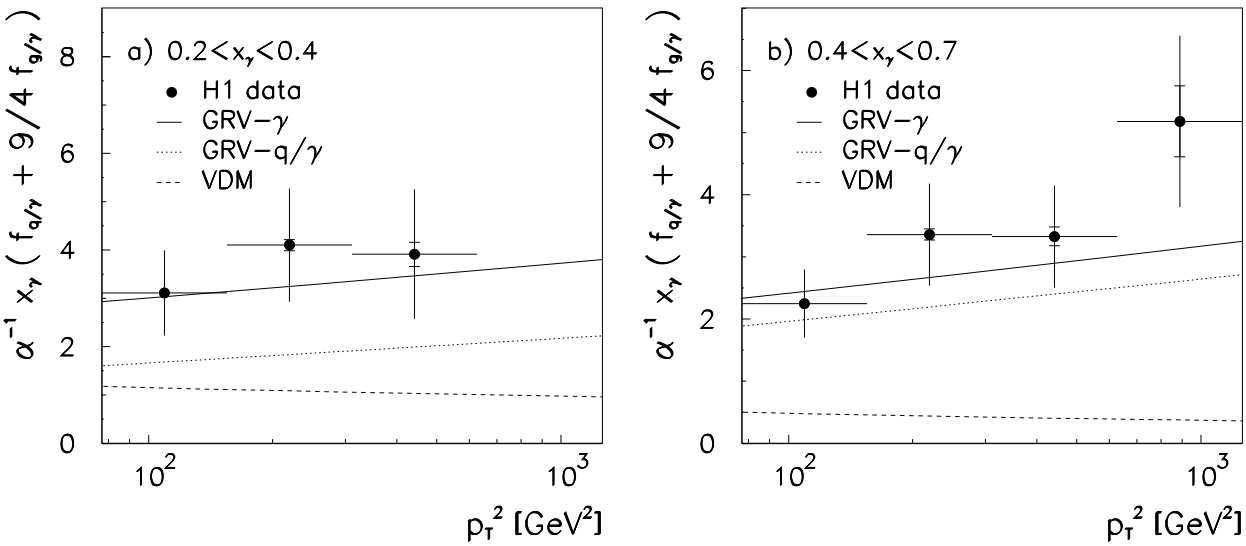

The hadron-like part is too low for all x, and the quark part is not sufficient $\Rightarrow$ gluons are needed.

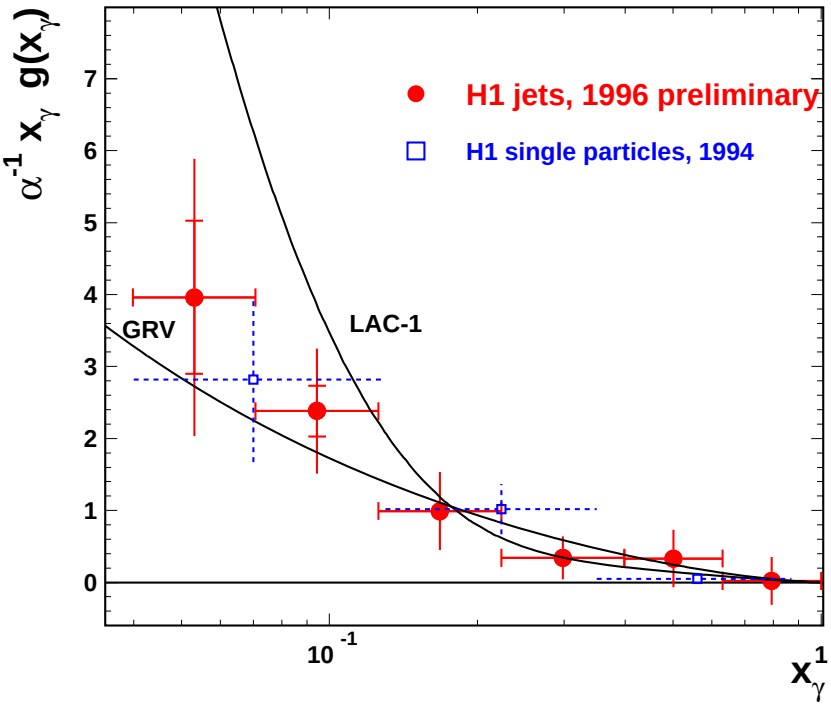

The gluon rises towards low x, and is small at large x

Structure of virtual photons from H1

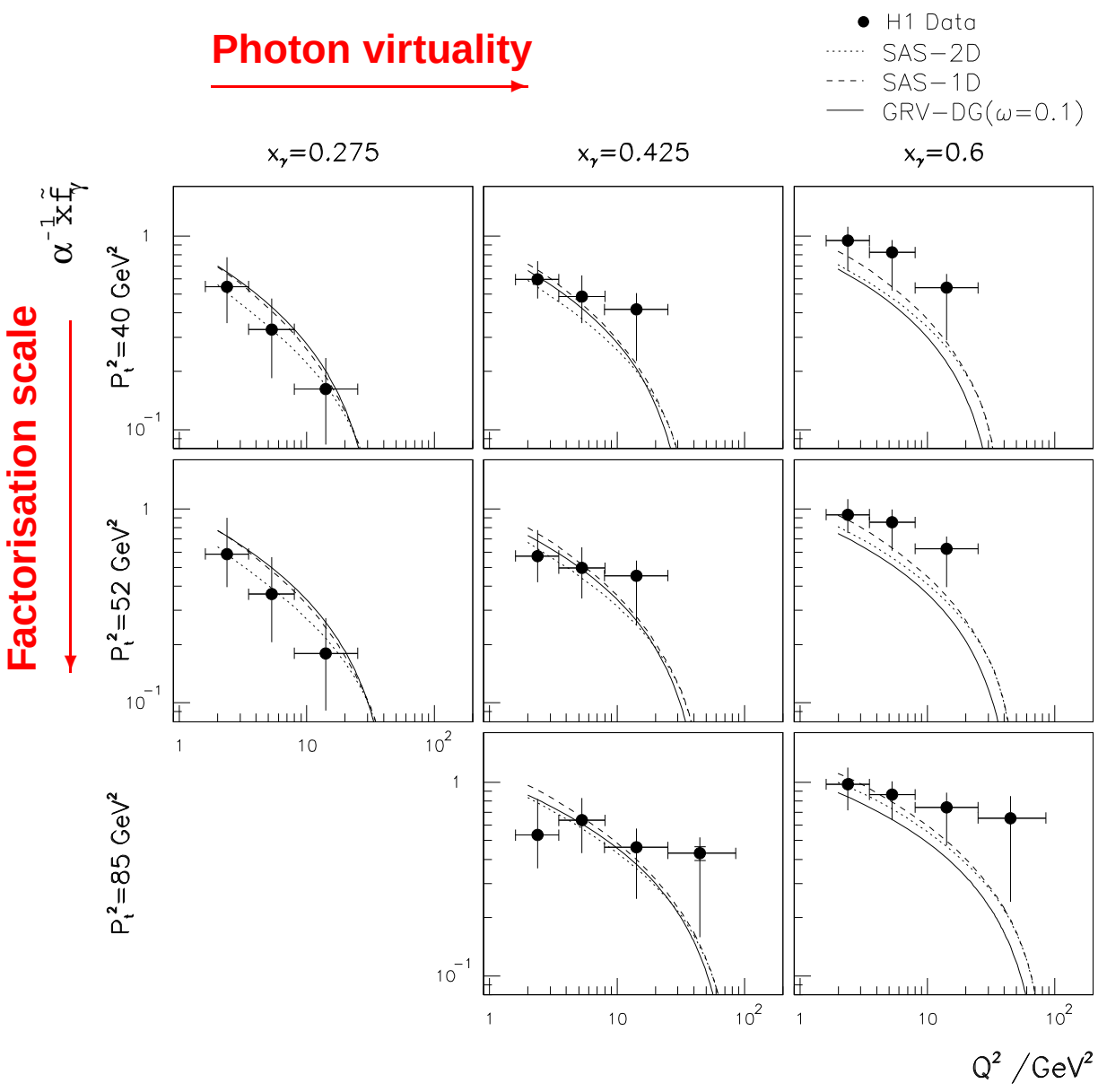

A strong suppression with increasing photon virtuality is observed.

Conclusions...

1. **QED is in good shape and successfully describes:**
   - (a) $F_{2,\mathrm{QED}}^{\gamma}$ in the large kinematical range of $1.5 < Q^2 < 400\ \mathrm{GeV}^2$ including the effect of the small virtuality of the quasi-real photon P^2.
   - (b) the structure functions F_{A}^{γ} and F_{B}^{γ}.
   - (c) the differential cross section $\mathrm{d}\sigma/\mathrm{d}x$ for $1.5 < P^2, Q^2 < 20, 30\ \mathrm{GeV}^2$.
2. **The hadronic structure is a field of active research.**
   - (a) Accurately describing the hadronic final state is non-trivial.
   - (b) The logarithmic rise of F_2^{γ} is clearly seen and the asymptotic solution is closer to the data than the QPM prediction.
   - (c) The low-x behaviour of F_2^{γ} is intensively studied.
   - (d) The first measurement of $F_{2,\mathrm{c}}^{\gamma}$ has been performed.
   - (e) The information on the structure of virtual photons is improved by a new measurement, but is still very limited.
3. **Photon-Photon Scattering:**
   - (a) Particle production and jet cross sections are described by NLO calculations, and $\sigma_{\mathrm{tot}}^{\gamma\gamma}$ is found to rise with W.

...continued

(a) The production of charm quarks has been measured, and is satisfactorily described by NLO calculations. The contributions from direct and resolved charm production are of similar size.

(b) The first measurement of bottom production has been performed.

1. Photon Structure from HERA:

(a) The measured jet cross-sections indicate a larger quark contribution to F_2^γ at medium to large x than is contained in present parametrisations. It remains to be seen whether both F_2^γ and the jet cross-sections can be accommodated in new global fits.

(b) The gluon distribution function of the photon rises towards low-x and is small at large-x.

(c) The structure of virtual photons is found to die out fast for increasing photon virtuality.

The general features of the photon structure are understood! Let us work on new and more precise results from LEP and HERA and plan for the future at a Linear Collider.

Slides: http://home.cern.ch/nisius